

# Carrollian correlators in black hole perturbation theory

Jiang Long<sup>1</sup>, Zhan-Jia Qu<sup>2</sup> & Hong-Yang Xiao<sup>3</sup>

*School of Physics, Huazhong University of Science and Technology,  
Luoyu Road 1037, Wuhan, Hubei 430074, China*

## Abstract

In this note, we clarify the relationship between the two-point Carrollian correlator and massless scattering in black hole background. It turns out that there are two kinds of Carrollian correlators at the null boundaries of each asymptotically flat spacetime. The correlator from  $\mathcal{I}^-$  to  $\mathcal{I}^+$  should be regularized by subtracting the flat space analog, and it is the position space version of the reflection amplitude of massless scattering. On the other hand, the correlator from  $\mathcal{I}^-$  to the future horizon  $\mathcal{H}^+$  is absent in flat space, and it is the position space version of the transmission amplitude. The poles of the Carrollian correlators are governed by the null geodesics from  $\mathcal{I}^-$  to  $\mathcal{I}^+$  or  $\mathcal{H}^+$ , and they define two kinds of classical equations in Carrollian space. These equations establish the relationship between the Shapiro time delay and the deflection angle for light rays and should be understood as the dual descriptions of the quasinormal modes (QNMs) and the branch cut of the Green's function. We find that the time delay contains a logarithmic/quadratic behavior for the correlator from  $\mathcal{I}^-$  to  $\mathcal{I}^+/\mathcal{H}^+$  for small deflection angles. On the other hand, the time delay is always increasing linearly for both correlators when the deflection angle is large.

---

<sup>1</sup>longjiang@hust.edu.cn

<sup>2</sup>m202470243@hust.edu.cn

<sup>3</sup>xiaohongyang@hust.edu.cn

# Contents

<b>1</b>	<b>Introduction</b>	<b>1</b>
<b>2</b>	<b>Carrollian correlator in black hole background</b>	<b>3</b>
2.1	Carrollian correlator in flat spacetime . . . . .	3
2.2	Carrollian correlator in Schwarzschild black hole background . . . . .	6
2.3	Approximation of the Carrollian correlator . . . . .	16
<b>3</b>	<b>Classical equations at null boundaries</b>	<b>20</b>
3.1	From $\mathcal{I}^-$ to $\mathcal{I}^+$ . . . . .	20
3.2	From $\mathcal{I}^-$ to $\mathcal{H}^+$ . . . . .	26
<b>4</b>	<b>Conclusion and discussion</b>	<b>29</b>
<b>A</b>	<b>Integration</b>	<b>32</b>
<b>B</b>	<b>The equation from <math>\mathcal{I}^-</math> to <math>\mathcal{I}^+</math></b>	<b>35</b>
<b>C</b>	<b>The equation from <math>\mathcal{I}^-</math> to <math>\mathcal{H}^+</math></b>	<b>41</b>

## 1 Introduction

Gravitational waves, ripples in spacetime that are predicted by general relativity and first detected by LIGO about a decade ago [1], are of great interest to astronomers since they are generated by some of the most energetic astrophysical processes, such as binary mergers, supernovae, and galaxy collisions. Due to their paramount importance in fundamental physics, various analytic methods, e.g., the Post-Newtonian (PN) expansion [2] and the effective one-body (EOB) formalism [3], have been developed to meet the needs of an upcoming era of high signal-to-noise ratio gravitational wave observations. In the PN regime, perturbative calculations are organized in terms of orders of velocity, and ideas from particle physics could play an important role. In the effective field theory (EFT) approach [4], the two body problem in gravity is converted to the computation of Feynman diagrams. Nowadays, advanced techniques from quantum field theory have been integrated into the Post-Minkowskian (PM) expansion of two body problems in general relativity [5].

In a parallel development, motivated by the success of AdS/CFT and asymptotic analysis [6–8] on gravitational physics near future/past null infinity ( $\mathcal{I}^\pm$ ), CFT techniques are applied to field theory at null boundary and lead to Carrollian holography [9]. Carrollian holography is a scenario of flat holography that maps the boundary Carrollian correlator to Carrollian amplitude [10–13], a position space scattering amplitude that can be computed perturbatively using the bulk-to-boundary propagator, bulk-to-bulk propagator as well as interaction vertices [14]. Most of the recent developments are restricted to theoretical exploration [15–19], and its connection to black hole physics is still under investigation. In the Carrollian framework, near-horizon black hole physics may be understood in the context of Carrollian hydrodynamics [20–26], which provides a macroscopic description based on Carrollian symmetry. One can also find the relationship between helicity flux and topological invariants on null hypersurfaces [27, 28]. Furthermore, the observational aspects have been explored for radiative systems [29, 30]. Unfortunately, these developments are relatively independent of the scattering amplitude approach based on the Carrollian correlator.

In principle, the Carrollian correlator should encode the crucial information of gravitational problems in position space, i.e. time domain physics and angle-dependent distributions of observables. In a recent paper [31], we propose to study thermal Carrollian correlators at null infinity and expect that they reveal a holographic description of black holes in asymptotically flat spacetimes. For technical reasons, we focus on the thermal Minkowski spacetime in that work. In this work, we will clarify the relationship between the Carrollian correlator and black hole perturbation theory. The latter is important for understanding Hawking radiation, black hole entropy, as well as astrophysical problems related to the detection of gravitational waves. To be more precise, we focus on the Green’s functions that are fundamental building blocks of black hole perturbation theory as well as of the Carrollian correlator. By extrapolating the Green’s function to  $\mathcal{I}^\pm$ , we obtain two kinds of two-point Carrollian correlators in a black hole background. The boundary-to-boundary correlator from  $\mathcal{I}^-$  to  $\mathcal{I}^+$  contains an IR regulator arising from the large radius that can be regularized by subtracting the flat space analog, leading to a Fourier transform of the scattering amplitude via the method of partial wave expansion. The other boundary-to-boundary correlator from  $\mathcal{I}^-$  to future event horizon  $\mathcal{H}^+$  is exactly the Fourier transform of the absorption amplitude. Physically, we expect that the poles of the two-point Carrollian correlators correspond to the null geodesics that emanate from  $\mathcal{I}^-$  and arrive at  $\mathcal{I}^+$  or  $\mathcal{H}^+$ . Thus we utilize the null geodesics to define classical equations at null boundaries. These equations impose constraints on the initial and final data for classical dynamics in the bulk. We analyze the asymptotic behaviour of the classical equations in detail.

The structure of this paper is as follows. In section 2, we derive the two-point Carrollian correlators in black hole perturbation theory. In section 3, we use the null geodesics in the bulk to define classical equations at null boundaries. We conclude with a summary and a discussion of future directions in the final section. Technical details of the integration and the proof of the properties of the classical equations are collected in three appendices.

## 2 Carrollian correlator in black hole background

In this section, we will first review the two-point Carrollian correlator in flat spacetime. Notations and conventions are introduced and the infrared problems in the flat space Carrollian correlator are discussed in the meantime. Then we delve into the two-point Carrollian correlator in black hole perturbation theory. A regularized Carrollian correlator is obtained by subtracting the flat space analog. We will also show that the Fourier transform of this regularized two-point Carrollian correlator is directly related to the scattering and absorption amplitude.

### 2.1 Carrollian correlator in flat spacetime

We focus on the four-dimensional Minkowski spacetime  $\mathbb{R}^{1,3}$  whose metric in Cartesian coordinates  $x^\mu = (t, \mathbf{x})$  is

$$ds^2 = \eta_{\mu\nu} dx^\mu dx^\nu = -dt^2 + dx^i dx^i, \quad \mu, \nu = 0, 1, 2, 3, \quad (2.1)$$

where the Minkowski matrix is  $\eta_{\mu\nu} = \text{diag}(-1, +1, +1, +1)$ . In spherical coordinates  $(t, r, \theta, \phi)$ , the metric is

$$ds^2 = -dt^2 + dr^2 + r^2(d\theta^2 + \sin^2 \theta d\phi^2). \quad (2.2)$$

To simplify notation, we will also collect the coordinates  $(\theta, \phi)$  as  $\Omega$ . Given a massless and real scalar field  $\Phi(x)$  in the bulk, we impose the fall-off condition

$$\Phi(x) = \begin{cases} \frac{\Sigma(u, \Omega)}{r} + \mathcal{O}(r^{-2}), & \text{near } \mathcal{I}^+ \\ \frac{\Sigma^{(-)}(v, \Omega)}{r} + \mathcal{O}(r^{-2}), & \text{near } \mathcal{I}^- \end{cases} \quad (2.3)$$

where the coefficients  $\Sigma(u, \Omega)$  and  $\Sigma^{(-)}(v, \Omega)$  are identified as boundary operators at  $\mathcal{I}^+$  and  $\mathcal{I}^-$ , respectively. The retarded coordinates  $(u = t - r, \Omega)$  are used in  $\mathcal{I}^+$  and the advanced coordinates  $(v = t + r, \Omega)$  are suitable for  $\mathcal{I}^-$ . The fundamental field  $\Sigma(u, \Omega)/\Sigma^{(-)}(v, \Omega)$  encodes the propagating degree of freedom of the bulk field and it is the leading order coefficient in the asymptotic expansion. In the language of the boundary Carrollian field theory, it is a primary operator on  $\mathcal{I}^\pm$  with dimension 1 and spin 0. The Feynman propagator in the bulk is defined in the conventional way

$$G_{\text{F}}(x; x') = \langle \text{T}\Phi(x)\Phi(x') \rangle \quad (2.4)$$

where  $\text{T}$  denotes the time-ordering operator

$$\text{T}\Phi(x)\Phi(x') = \Theta(x^0 - x'^0)\Phi(x)\Phi(x') + \Theta(x'^0 - x^0)\Phi(x')\Phi(x). \quad (2.5)$$

By extrapolating one of the bulk field to the boundary, we obtain the retarded and advanced bulk-to-boundary propagators as follows:

$$D(u, \Omega; x') = \langle \Sigma(u, \Omega)\Phi(x') \rangle = \lim_{r \rightarrow \mathcal{I}^+} r G_{\text{F}}(x; x'), \quad (2.6a)$$

$$D^{(-)}(v', \Omega'; x) = \langle \Phi(x) \Sigma^{(-)}(v', \Omega') \rangle = \lim_{r' \rightarrow \mathcal{I}^-} r' G_F(x; x'). \quad (2.6b)$$

The symbol  $\lim_{r \rightarrow \mathcal{I}^+}$  means to take the limit by moving  $r \rightarrow \infty$  and keeping  $u$  finite at the same time. Similarly, the symbol  $\lim_{r \rightarrow \mathcal{I}^-}$  means to take the limit by moving  $r \rightarrow \infty$  and keeping  $v$  finite at the same time. The complex conjugate of the Feynman propagator is called the anti-Feynman propagator

$$G_{\bar{F}}(x; x') = \langle \bar{\mathbb{T}}\Phi(x)\Phi(x') \rangle = (G_F(x; x'))^* \quad (2.7)$$

where  $\bar{\mathbb{T}}$  denotes the anti-time ordering operator

$$\bar{\mathbb{T}}\Phi(x)\Phi(x') = \Theta(x^0 - x'^0)\Phi(x')\Phi(x) + \Theta(x'^0 - x^0)\Phi(x)\Phi(x'). \quad (2.8)$$

Thus we can also obtain the complex conjugate of the retarded and advanced bulk-to-boundary propagators

$$D^*(u, \Omega; x') = \langle \Phi(x') \Sigma(u, \Omega) \rangle = \lim_{r \rightarrow \mathcal{I}^+} r G_{\bar{F}}(x; x'), \quad (2.9a)$$

$$D^{(-)*}(v', \Omega'; x) = \langle \Sigma^{(-)}(v', \Omega') \Phi(x) \rangle = \lim_{r' \rightarrow \mathcal{I}^-} r' G_{\bar{F}}(x; x'). \quad (2.9b)$$

From the Feynman propagator

$$G_F(x; x') = \frac{1}{4\pi^2} \frac{1}{(x - x')^2 + i\epsilon}, \quad (2.10)$$

it is straightforward to obtain the retarded and advanced bulk-to-boundary correlators

$$D(u, \Omega; x') = -\frac{1}{8\pi^2(u + n \cdot x' - i\epsilon)}, \quad (2.11a)$$

$$D^{(-)}(v', \Omega'; x) = \frac{1}{8\pi^2(v' - \bar{n}' \cdot x + i\epsilon)}. \quad (2.11b)$$

The null vector  $n^\mu$  is determined by the  $\Omega$

$$n^\mu = (1, \sin \theta \cos \phi, \sin \theta \sin \phi, \cos \theta) = (1, n^i) \quad (2.12)$$

while

$$\bar{n}'^\mu = (-1, \sin \theta' \cos \phi', \sin \theta' \sin \phi', \cos \theta') = (-1, n'^i). \quad (2.13)$$

The unit vector  $n^i$  is the normal vector of the  $S^2$  by embedding it into  $\mathbb{R}^3$ . The boundary-to-boundary propagator is formally obtained by extrapolating the remaining field to the boundary

$$B(u, \Omega; v', \Omega') = \langle \Sigma(u, \Omega) \Sigma^{(-)}(v', \Omega') \rangle = \lim_{r' \rightarrow \mathcal{I}^-} r' D(u, \Omega; x'). \quad (2.14)$$

Note that one should get the same result via the alternative formula

$$B^{(-)}(u, \Omega; v', \Omega') = \langle \Sigma(u, \Omega) \Sigma^{(-)}(v', \Omega') \rangle = \lim_{r \rightarrow \mathcal{I}^+} r D^{(-)}(v', \Omega'; x). \quad (2.15)$$

This has been evaluated in [31] and we have obtained the electric and magnetic branch. However, the parameter in the  $i\epsilon$  prescription of the magnetic branch depends on the infrared radius slightly. To clarify this point, we work in the integral representation of the bulk-to-boundary propagator

$$D(u, \Omega; x') = \frac{i}{8\pi^2} \int_0^\infty d\omega e^{-i\omega(u+n \cdot x' - i\epsilon)} \quad (2.16)$$

Note that  $n \cdot x' = -v' + r'n \cdot \bar{n}'$ , we use the identity

$$e^{-i\omega r'n \cdot \bar{n}'} = e^{-i\omega r' - i\omega r' n \cdot \mathbf{n}'} = e^{-i\omega r'} 4\pi \sum_{\ell, m} (-i)^\ell j_\ell(\omega r') Y_{\ell, m}(\Omega) Y_{\ell, m}^*(\Omega') \quad (2.17)$$

and then the large  $r'$  expansion of the exponential function is

$$e^{-i\omega r'n \cdot \bar{n}'} = \frac{4\pi}{2i\omega r'} \sum_{\ell, m} (-1)^\ell Y_{\ell, m}(\Omega) Y_{\ell, m}^*(\Omega') - \frac{4\pi}{2i\omega r'} e^{-2i\omega r'} \sum_{\ell, m} Y_{\ell, m}(\Omega) Y_{\ell, m}^*(\Omega') + \mathcal{O}(r'^{-2}). \quad (2.18)$$

The boundary-to-boundary propagator (2.14) is

$$\begin{aligned} B(u, \Omega; v', \Omega') &= -\frac{1}{4\pi} \int_0^\infty \frac{d\omega}{\omega} e^{-i\omega(u-v')} \sum_{\ell, m} (-1)^\ell Y_{\ell, m}(\Omega) Y_{\ell, m}^*(\Omega') \\ &\quad + \frac{1}{4\pi} \int_0^\infty \frac{d\omega}{\omega} e^{-i\omega(u-v'+2r')} \sum_{\ell, m} Y_{\ell, m}(\Omega) Y_{\ell, m}^*(\Omega'). \end{aligned} \quad (2.19)$$

Note that the second line depends on the infrared radius  $r' \rightarrow \infty$  explicitly. One may ignore this term to obtain the two-point Carrollian correlator in the electric branch. However, a much more careful treatment of this term would give us a magnetic branch [31]. In this work, we will leave it in this form for later convenience. Rather interesting, we can also use the formula (2.15) to obtain the two-point correlator

$$\begin{aligned} B^{(-)}(u, \Omega; v', \Omega') &= -\frac{1}{4\pi} \int_0^\infty \frac{d\omega}{\omega} e^{-i\omega(u-v')} \sum_{\ell, m} (-1)^\ell Y_{\ell, m}(\Omega) Y_{\ell, m}^*(\Omega') \\ &\quad + \frac{1}{4\pi} \int_0^\infty \frac{d\omega}{\omega} e^{-i\omega(u-v'+2r)} \sum_{\ell, m} Y_{\ell, m}(\Omega) Y_{\ell, m}^*(\Omega'). \end{aligned} \quad (2.20)$$

By definition, the two-point correlator  $B^{(-)}$  is formally the same as  $B$ . However, the result depends on the description since the infrared radius in (2.20) is  $r$  while it is  $r'$  in (2.19). One may identify  $r = r'$  to get the same result. It is a bit confusing that why the two different radius should be identical. In the following, we will find that the paradoxical term should be subtracted in black hole perturbation theory and there is no need to identify  $r$  and  $r'$ .

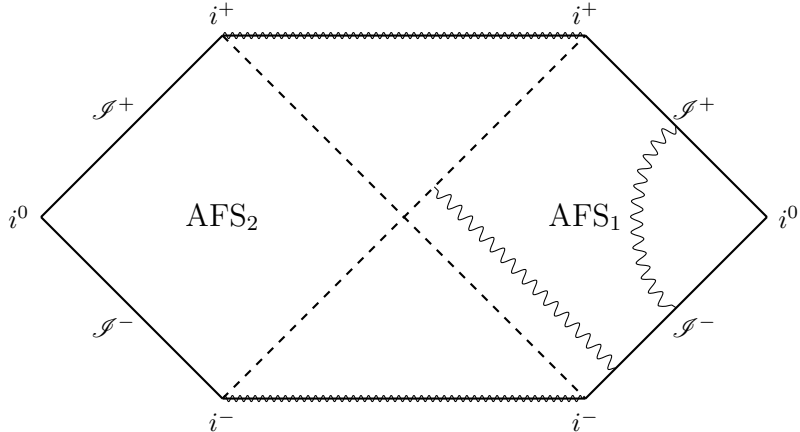


**Figure 1:** Penrose diagram of two-side Schwarzschild black hole and Carrollian propagators in an asymptotically flat region.

## 2.2 Carrollian correlator in Schwarzschild black hole background

In this subsection, we will initiate a definition of Carrollian correlator in an asymptotically flat spacetime. For the sake of clarity, we will focus on the two-point Carrollian correlator of massless scalar theory in Schwarzschild background. The Penrose diagram of two-side Schwarzschild black hole is shown in figure 1, we will focus on the physically relevant region  $\text{AFS}_1$ . Considering a  $1 \rightarrow 1$  scattering problem in Schwarzschild background, the incoming wave is from  $\mathcal{I}^-$  and into the future. Part of the wave is scattered by the black hole and becomes the outgoing wave at  $\mathcal{I}^+$ . The remaining wave is absorbed by the black hole and becomes the ingoing wave at the future event horizon  $\mathcal{H}^+$ . There is no wave coming from the past event horizon  $\mathcal{H}^-$ . Thus we will discuss Carrollian correlator from  $\mathcal{I}^-$  to  $\mathcal{I}^+$  or  $\mathcal{H}^+$ . The two kinds of correlator are also shown in figure 1.

The Klein-Gordon equation in Schwarzschild background is

$$\square\Phi = 0 \tag{2.21}$$

and one can solve it by separation of variables

$$\Phi(x) = \int d\omega e^{-i\omega t} \sum_{\ell, m} \frac{1}{r} u_{\omega, \ell}(r) Y_{\ell, m}(\Omega) \tag{2.22}$$

where we have inserted a factor  $r^{-1}$  in the expansion to adapt to the fall-off behaviour (2.3).

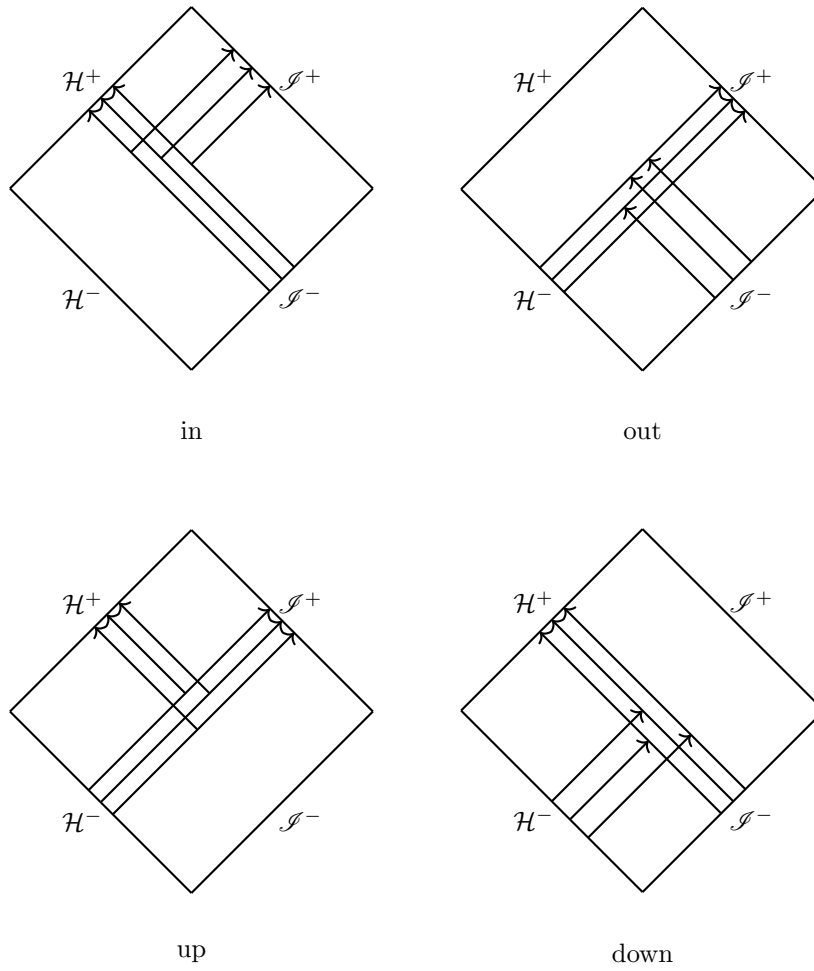


**Figure 2:** An illustration of the boundary conditions for the in, out, up and down modes.

The function  $u_{\omega,\ell}(r)$  satisfies the second order differential equation<sup>4</sup>

$$\frac{d^2}{dr_*^2} u_{\omega,\ell} + [\omega^2 - V_\ell(r)] u_{\omega,\ell} = 0 \quad (2.23)$$

where  $V_\ell$  is the potential

$$V_\ell(r) = \left(1 - \frac{2M}{r}\right) \left(\frac{\ell(\ell+1)}{r^2} + \frac{2M}{r^3}\right). \quad (2.24)$$

In this expression,  $M$  is the mass of the black hole and  $\ell = 0, 1, 2, \dots$  is the quantum number of angular momentum. The tortoise coordinate  $r_*$  is determined by the equation

$$\frac{dr_*}{dr} = \frac{1}{1 - \frac{2M}{r}} \Rightarrow r_*(r) = \int_o^r dr' \left(1 - \frac{2M}{r'}\right)^{-1} \quad (2.25)$$

up to a reference point  $o$ . The conventional choice is

$$r_*(r) = r + 2M \ln \left(\frac{r}{2M} - 1\right). \quad (2.26)$$

However, the other choice is also fine. In general, we have

$$r_*(r) = r - o + 2M \ln \frac{r - 2M}{o - 2M}. \quad (2.27)$$

To recover the standard  $r_*$ , the reference point  $o = 2M\zeta$  should obey the equation

$$\zeta + \ln(\zeta - 1) = 0 \Rightarrow \zeta \approx 1.2785. \quad (2.28)$$

The equation (2.23) can be solved by imposing suitable boundary condition. In figure 2, we have shown four kinds of modes according to the boundary conditions. The corresponding solutions are denoted as  $u_{\omega,\ell}^{\text{in}}, u_{\omega,\ell}^{\text{out}}, u_{\omega,\ell}^{\text{up}}, u_{\omega,\ell}^{\text{down}}$  respectively. As an illustration, the “in” mode obeys the boundary condition

$$u_{\omega,\ell}^{\text{in}} \sim \begin{cases} e^{-i\omega r_*}, & r_* \rightarrow -\infty \\ A_{\omega,\ell}^{\text{in,up}} e^{i\omega r_*} + A_{\omega,\ell}^{\text{in,down}} e^{-i\omega r_*}, & r_* \rightarrow \infty. \end{cases} \quad (2.29)$$

The coefficients  $A_{\omega,\ell}^{\text{in,up}}$  and  $A_{\omega,\ell}^{\text{in,down}}$  are determined by solving the equation near the horizon and extend it to null infinities. In black hole scattering problems, the transmission and reflection amplitude are defined via

$$\mathcal{T}_{\omega,\ell} = \frac{1}{A_{\omega,\ell}^{\text{in,down}}}, \quad \mathcal{R}_{\omega,\ell} = \frac{A_{\omega,\ell}^{\text{in,up}}}{A_{\omega,\ell}^{\text{in,down}}} \quad (2.30)$$

---

<sup>4</sup>This is the Regge-Wheeler-Zerilli type equation [32, 33]. In black hole perturbation theory, the related wave equation for a Weyl scalar in Newman-Penrose formalism [34] is called the Teukolsky equation [35]. More general formalism can be found in [36].

and they satisfy the standard scattering relation

$$|\mathcal{T}_{\omega,\ell}|^2 + |\mathcal{R}_{\omega,\ell}|^2 = 1. \quad (2.31)$$

Note that only two of the modes are linearly independent in general. By matching the boundary conditions, we may write

$$u_{\omega,\ell}^{\text{in}} = A_{\omega,\ell}^{\text{in,up}} u_{\omega,\ell}^{\text{up}} + A_{\omega,\ell}^{\text{in,down}} u_{\omega,\ell}^{\text{down}}. \quad (2.32)$$

The transmission and reflection amplitude can be obtained by solving the retarded Green's function  $G_R(x; x')$

$$\square G_R(x; x') = \frac{i}{\sqrt{-g}} \delta^{(4)}(x - x') \quad (2.33)$$

that satisfies the ingoing boundary condition at  $\mathcal{H}^+$  and outgoing boundary condition at  $\mathcal{S}^+$  together with the condition  $G_R(x; x') = 0$  for  $t < t'$ . Expanding the Green's function via the eigenfunctions

$$G_R(x; x') = -\frac{i}{2\pi r r'} \int_{\mathcal{C}} d\omega e^{-i\omega(t-t')} \sum_{\ell,m} G_{\omega,\ell}(r; r') Y_{\ell,m}(\Omega) Y_{\ell,m}^*(\Omega'), \quad (2.34)$$

the radial function  $G_{\omega,\ell}(r; r')$  can be constructed through the “in” and ”up” modes

$$G_{\omega,\ell}(r; r') = \frac{u_{\omega,\ell}^{\text{in}}(r_{<}) u_{\omega,\ell}^{\text{up}}(r_{>})}{W_{\omega,\ell}} \quad (2.35)$$

where  $r_{>} = \max\{r, r'\}$  and  $r_{<} = \min\{r, r'\}$ . The Wronskian  $W_{\omega,\ell}$  is defined as

$$W_{\omega,\ell} = u_{\omega,\ell}^{\text{up}} \partial_r u_{\omega,\ell}^{\text{in}} - u_{\omega,\ell}^{\text{in}} \partial_r u_{\omega,\ell}^{\text{up}} \quad (2.36)$$

and it is independent of  $r$  and  $r'$

$$W_{\omega,\ell} = -2i\omega A_{\omega,\ell}^{\text{in,down}}. \quad (2.37)$$

The integral of (2.34) is evaluated by considering a contour  $\mathcal{C}$  that is displaced slightly above the real  $\omega$  axis, e.g.,

$$G_R(x; x') = -\frac{i}{2\pi r r'} \int_{-\infty+i\epsilon}^{\infty+i\epsilon} d\omega e^{-i\omega(t-t')} \sum_{\ell,m} G_{\omega,\ell}(r; r') Y_{\ell,m}(\Omega) Y_{\ell,m}^*(\Omega'). \quad (2.38)$$

As a function of complex frequency,  $G_{\omega,\ell}$  has an infinite tower of quasi-normal modes (QNMs) located at the lower half plane [37]. These modes are determined by the zeros of the Wronskian

$$W_{\omega,\ell} \Big|_{\omega=\omega_{QNM}} = 0. \quad (2.39)$$

As a matter of fact, there is also a branch cut along the imaginary axis [38, 39]. Now we use (2.38) and (2.35) to define the bulk-to-boundary propagators

$$D_R(u, \Omega; x') = \lim_{r \rightarrow \mathcal{I}^+} r G_R(x; x'), \quad (2.40a)$$

$$D_R^{(-)}(v', \Omega'; x) = \lim_{r' \rightarrow \mathcal{I}^-} r' G_R(x; x'), \quad (2.40b)$$

$$D_R^{\mathcal{H}^+}(v, \Omega; x') = \lim_{r \rightarrow \mathcal{H}^+} r G_R(x; x'), \quad (2.40c)$$

$$D_R^{\mathcal{H}^-}(u', \Omega'; x) = \lim_{r' \rightarrow \mathcal{H}^-} r' G_R(x; x'). \quad (2.40d)$$

More precisely,

$$D_R(u, \Omega; x') = \frac{1}{4\pi r'} \int_{-\infty+i\epsilon}^{\infty+i\epsilon} \frac{d\omega}{\omega} e^{-i\omega(u-t')} \sum_{\ell, m} \mathcal{T}_{\omega, \ell} u_{\omega, \ell}^{\text{in}}(r') Y_{\ell, m}(\Omega) Y_{\ell', m'}^*(\Omega'), \quad (2.41a)$$

$$D_R^{(-)}(v', \Omega'; x) = \frac{1}{4\pi r} \int_{-\infty+i\epsilon}^{\infty+i\epsilon} \frac{d\omega}{\omega} e^{-i\omega(t-v')} \sum_{\ell, m} \mathcal{T}_{\omega, \ell} u_{\omega, \ell}^{\text{in}}(r) Y_{\ell, m}(\Omega) Y_{\ell, m}^*(\Omega'), \quad (2.41b)$$

$$D_R^{\mathcal{H}^+}(v, \Omega; x') = \frac{1}{4\pi r'} \int_{-\infty+i\epsilon}^{\infty+i\epsilon} \frac{d\omega}{\omega} e^{-i\omega(v-t')} \sum_{\ell, m} \mathcal{T}_{\omega, \ell} u_{\omega, \ell}^{\text{up}}(r') Y_{\ell, m}(\Omega) Y_{\ell, m}^*(\Omega'), \quad (2.41c)$$

$$D_R^{\mathcal{H}^-}(u', \Omega'; x) = 0. \quad (2.41d)$$

The last bulk-to-boundary correlator vanishes since the solution  $u^{\text{in}}$  vanishes at  $\mathcal{H}^-$ . In all the expressions, we have added a subscript  $R$  to distinguish them with the advanced/retarded bulk-to-boundary propagator in previous subsection. Here the bulk-to-boundary correlators are extracted from the retarded Green's function in the bulk. However, the advanced/retarded bulk-to-boundary propagators are extracted from the Feynman propagator in the bulk. Note that the retarded Green's function is related to the Feynman propagator via

$$G_R(x; x') = \theta(x^0 - x'^0) \langle [\Phi(x), \Phi(x')] \rangle = \theta(x^0 - x'^0) (G_F(x; x') - G_{\bar{F}}(x; x')) = 2i\theta(x^0 - x'^0) \text{Im} G_F(x; x'). \quad (2.42)$$

Therefore, the flat spacetime analogs of  $D_R$  are

$$D_R^0(u, \Omega; x') = \lim_{r \rightarrow \mathcal{I}^+} r G_R^0(x; x') = \frac{i}{8\pi^2} \int_{-\infty}^{\infty} d\omega e^{-i\omega(u+n \cdot x')}, \quad (2.43a)$$

$$D_R^{(-)0}(v', \Omega'; x) = \lim_{r' \rightarrow \mathcal{I}^-} r' G_R^0(x; x') = \frac{i}{8\pi^2} \int_{-\infty}^{\infty} d\omega e^{i\omega(v' - \bar{n}' \cdot x)}. \quad (2.43b)$$

Here we add a superscript 0 to denote the result in flat spacetime. The bulk-to-future horizon  $\mathcal{H}^+$  propagator is absent in the flat spacetime. By extrapolating the remaining field to the null boundary in (2.41), we may define the following boundary-to-boundary commutators

$$B_R(u, \Omega; v', \Omega') = \lim_{r' \rightarrow \mathcal{I}^-} r' D_R(u, \Omega; x') = \lim_{r' \rightarrow \mathcal{I}^-} \lim_{r \rightarrow \mathcal{I}^+} r r' G_R(x; x'), \quad (2.44a)$$

$$B_R^{(-)}(u, \Omega; v', \Omega') = \lim_{r \rightarrow \mathcal{I}^+} r D_R^{(-)}(v', \Omega'; x) = \lim_{r \rightarrow \mathcal{I}^+} \lim_{r' \rightarrow \mathcal{I}^-} r r' G_R(x; x'), \quad (2.44b)$$

$$B_R^{(-), \mathcal{H}^+}(v, \Omega; v', \Omega') = \lim_{r \rightarrow \mathcal{H}^+} r D_R^{(-)}(v', \Omega'; x) = \lim_{r \rightarrow \mathcal{H}^+} \lim_{r' \rightarrow \mathcal{I}^-} r r' G_R(x; x'), \quad (2.44c)$$

$$B_R^{\mathcal{H}^+, (-)}(v, \Omega; v', \Omega') = \lim_{r' \rightarrow \mathcal{I}^-} r' D_R^{\mathcal{H}^+}(v, \Omega; x') = \lim_{r' \rightarrow \mathcal{I}^-} \lim_{r \rightarrow \mathcal{H}^+} r r' G_R(x; x'). \quad (2.44d)$$

Assuming the double limits commute with each other, we may obtain the following identities

$$B_R(u, \Omega; v', \Omega') = B_R^{(-)}(u, \Omega; v', \Omega'), \quad (2.45a)$$

$$B_R^{(-), \mathcal{H}^+}(v, \Omega; v', \Omega') = B_R^{\mathcal{H}^+, (-)}(v, \Omega; v', \Omega'). \quad (2.45b)$$

To check them, we evaluate the limits explicitly,

$$B_R(u, \Omega; v', \Omega') = \frac{1}{4\pi} \int_{-\infty+i\epsilon}^{\infty+i\epsilon} \frac{d\omega}{\omega} \sum_{\ell, m} \left( e^{-i\omega(u-v')} \mathcal{R}_{\omega, \ell} + e^{-i\omega(u-u')} \right) Y_{\ell, m}(\Omega) Y_{\ell, m}^*(\Omega'), \quad (2.46a)$$

$$B_R^{(-)}(u, \Omega; v', \Omega') = \frac{1}{4\pi} \int_{-\infty+i\epsilon}^{\infty+i\epsilon} \frac{d\omega}{\omega} \sum_{\ell, m} \left( e^{-i\omega(u-v')} \mathcal{R}_{\omega, \ell} + e^{-i\omega(v-v')} \right) Y_{\ell, m}(\Omega) Y_{\ell, m}^*(\Omega'), \quad (2.46b)$$

$$B_R^{(-), \mathcal{H}^+}(v, \Omega; v', \Omega') = \frac{1}{4\pi} \int_{-\infty+i\epsilon}^{\infty+i\epsilon} \frac{d\omega}{\omega} e^{-i\omega(v-v')} \sum_{\ell, m} \mathcal{T}_{\omega, \ell} Y_{\ell, m}(\Omega) Y_{\ell, m}^*(\Omega'), \quad (2.46c)$$

$$B_R^{\mathcal{H}^+, (-)}(v, \Omega; v', \Omega') = \frac{1}{4\pi} \int_{-\infty+i\epsilon}^{\infty+i\epsilon} \frac{d\omega}{\omega} e^{-i\omega(v-v')} \sum_{\ell, m} \mathcal{T}_{\omega, \ell} Y_{\ell, m}(\Omega) Y_{\ell, m}^*(\Omega'). \quad (2.46d)$$

Interestingly, the second identity (2.45b) is satisfied while the first identity (2.45a) is not valid. The mismatch between  $B_R$  and  $B_R^{(-)}$  is from the highly oscillating terms that depend on the IR regulators. These terms remind us the similar behaviour of (2.19) and (2.20) in flat spacetime. In fact, we can also define the boundary commutators from (2.43)

$$B_R^0(u, \Omega; v', \Omega') = -\frac{1}{4\pi} \int_{-\infty+i\epsilon}^{\infty+i\epsilon} \frac{d\omega}{\omega} \sum_{\ell, m} \left( e^{-i\omega(u-v')} (-1)^\ell - e^{-i\omega(u-u')} \right) Y_{\ell, m}(\Omega) Y_{\ell, m}^*(\Omega'), \quad (2.47a)$$

$$B_R^{(-), 0}(u, \Omega; v', \Omega') = -\frac{1}{4\pi} \int_{-\infty+i\epsilon}^{\infty+i\epsilon} \frac{d\omega}{\omega} \sum_{\ell, m} \left( e^{-i\omega(u-v')} (-1)^\ell - e^{-i\omega(v-v')} \right) Y_{\ell, m}(\Omega) Y_{\ell, m}^*(\Omega'). \quad (2.47b)$$

Both of them are formally equal to  $\langle [\Sigma(u, \Omega), \Sigma^{(-)}(v', \Omega')] \rangle$  while they actually depend on the IR regulators. Note that the dependence on the IR regulator is exactly the same in Schwarzschild and flat spacetime. We may subtract the flat spacetime correlator from the corresponding one

in the Schwarzschild spacetime and get a unique boundary-to-boundary correlator from  $\mathcal{I}^-$  to  $\mathcal{I}^+$

$$C(u, \Omega; v', \Omega') = B_R(u, \Omega; v', \Omega') - B_R^0(u, \Omega; v', \Omega') = B_R^{(-)}(u, \Omega; v', \Omega') - B_R^{(-),0}(u, \Omega; v', \Omega'). \quad (2.48)$$

More precisely,

$$\begin{aligned} C(u, \Omega; v', \Omega') &= \frac{1}{4\pi} \int_{-\infty+i\epsilon}^{\infty+i\epsilon} \frac{d\omega}{\omega} e^{-i\omega(u-v')} \sum_{\ell, m} (\mathcal{R}_{\omega, \ell} + (-1)^\ell) Y_{\ell, m}(\Omega) Y_{\ell, m}^*(\Omega') \\ &= -\frac{1}{16\pi^2} \int_{-\infty+i\epsilon}^{\infty+i\epsilon} \frac{d\omega}{\omega} e^{-i\omega(u-v')} \sum_{\ell} (2\ell + 1) (e^{2i\delta_\ell} - 1) P_\ell(\cos \gamma^P). \end{aligned} \quad (2.49)$$

In the second step, we have used the spherical symmetry and the addition theorem

$$\sum_{m=-\ell}^{\ell} Y_{\ell, m}(\Omega) Y_{\ell, m}^*(\Omega') = \frac{2\ell + 1}{4\pi} P_\ell(\cos \gamma) \quad (2.50)$$

where  $P_\ell(\cos \gamma)$  is the Legendre polynomial of order  $\ell$  and  $\gamma$  is the angle between the directions  $\Omega$  and  $\Omega'$ . Note that in (2.49) the angle is denoted as  $\gamma^P$  which means the angle between  $\Omega^P$  and  $\Omega'$ . There is a factor  $(-1)^\ell$  in the summation and its effect is to map  $\Omega$  to its antipodal point  $\Omega^P$ . We have also rewritten the reflection amplitude  $\mathcal{R}_{\omega, \ell}$  through a phase shift factor

$$e^{2i\delta_\ell} = (-1)^{\ell+1} \mathcal{R}_{\omega, \ell}. \quad (2.51)$$

Interestingly, the summation of  $\ell$  is exactly equal to the scattering amplitude  $f(\gamma)$  in the partial wave expansion

$$f(\omega, \gamma) = \frac{1}{2i\omega} \sum_{\ell} (2\ell + 1) (e^{2i\delta_\ell} - 1) P_\ell(\cos \gamma) \quad (2.52)$$

and then the correlator from  $\mathcal{I}^-$  to  $\mathcal{I}^+$  is the Fourier transform of the scattering amplitude

$$C(u, \Omega; v', \Omega'^P) = -\frac{i}{8\pi^2} \int_{-\infty+i\epsilon}^{\infty+i\epsilon} d\omega e^{-i\omega(u-v')} f(\omega, \gamma). \quad (2.53)$$

Inversely, the scattering amplitude is

$$f(\omega, \gamma) = 4\pi i \int_{-\infty}^{\infty} du e^{i\omega u} C(u, \Omega; 0, \Omega'^P). \quad (2.54)$$

We have used the time translation symmetry to set  $v' = 0$  on the right hand side. In particular, the zero frequency limit of the scattering amplitude is proportional to the ‘‘average null’’ Carrollian correlator from  $\mathcal{I}^-$  to  $\mathcal{I}^+$

$$f(0, \gamma) = 4\pi i \int_{-\infty}^{\infty} du C(u, \Omega; 0, \Omega'^P). \quad (2.55)$$

The scattering cross section is

$$\frac{d\sigma_{\text{sca}}}{d\Omega} = |f(\omega, \gamma)|^2 = 16\pi^2 \left| \int_{-\infty}^{\infty} du e^{i\omega u} C(u, \Omega; 0, \Omega'^P) \right|^2. \quad (2.56)$$

The formula connects the Carrollian correlator to the scattering cross section in black hole perturbation theory.

Now we explore the other Carrollian correlator from  $\mathcal{I}^-$  to  $\mathcal{H}^+$

$$\begin{aligned} \tilde{C}(v, \Omega; v', \Omega') &= B_R^{(-), \mathcal{H}^+}(v, \Omega; v', \Omega') = B_R^{\mathcal{H}^+, (-)}(v, \Omega; v', \Omega') \\ &= \frac{i}{8\pi^2} \int_{-\infty+i\epsilon}^{\infty+i\epsilon} d\omega e^{-i\omega(v-v')} \tilde{f}(\omega, \gamma) \end{aligned} \quad (2.57)$$

where  $\tilde{f}(\omega, \gamma)$  is the absorption amplitude

$$\tilde{f}(\omega, \gamma) = \frac{1}{2i\omega} \sum_{\ell} (2\ell + 1) \mathcal{T}_{\omega, \ell} P_{\ell}(\cos \gamma) \quad (2.58)$$

which is determined by the transmission amplitude  $\mathcal{T}_{\omega, \ell}$ . We find its connection to the Carrollian correlator as

$$\tilde{f}(\omega, \gamma) = -4\pi i \int_{-\infty}^{\infty} dv e^{i\omega v} \tilde{C}(v, \Omega; 0, \Omega'). \quad (2.59)$$

In the zero frequency limit, this is the ‘‘average null’’ Carrollian correlator from  $\mathcal{I}^-$  to  $\mathcal{H}^+$

$$\tilde{f}(0, \gamma) = -4\pi i \int_{-\infty}^{\infty} dv \tilde{C}(v, \Omega; 0, \Omega'). \quad (2.60)$$

The absorption cross section is

$$\frac{d\sigma_{\text{abs}}}{d\Omega} = |\tilde{f}(\omega, \gamma)|^2 = 16\pi^2 \left| \int_{-\infty}^{\infty} dv e^{i\omega v} \tilde{C}(v, \Omega; 0, \Omega') \right|^2. \quad (2.61)$$

The absorption cross section is proportional to the area of the event horizon for a spherically symmetric black hole in an asymptotically flat spacetime [40–45]. Therefore, we obtain the following universal result for Carrollian correlator

$$\left| \int_{-\infty}^{\infty} dv \tilde{C}(v, \Omega; 0, \Omega') \right|^2 \propto \text{Area of the event horizon}. \quad (2.62)$$

The left hand side is the square of the ‘‘average null’’ Carrollian correlator from  $\mathcal{I}^-$  to  $\mathcal{H}^+$ . We conclude that the ‘‘average null’’ Carrollian correlator  $\tilde{C}$  has a geometric meaning and is also related to the entropy of the black hole. More properties of the Carrollian correlators are discussed in the following:

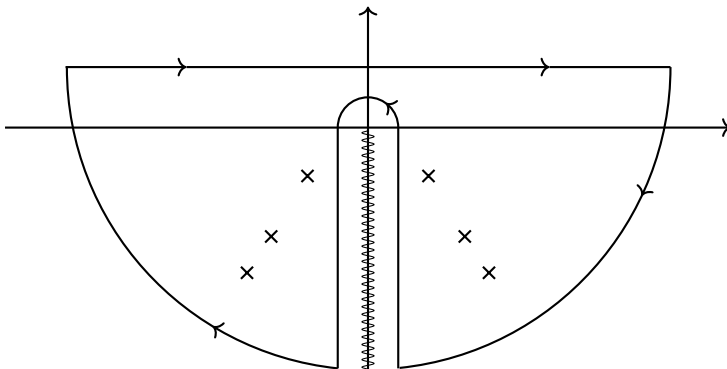


**Figure 3:** Contour for region  $\mathcal{S}_L^+$ . The QNMs are labeled by small  $\times$  and the branch cut is represented by wavy lines.

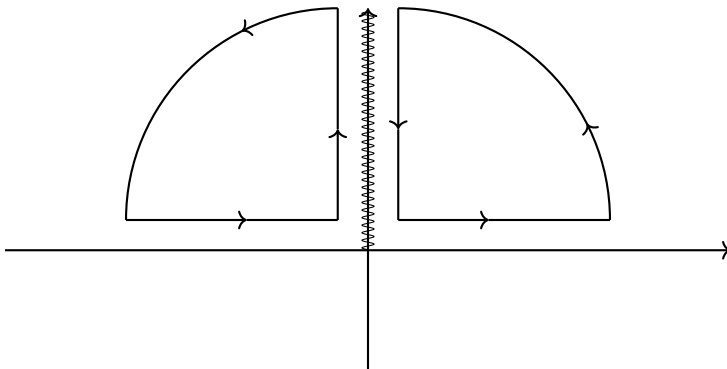


**Figure 4:** Contour for region  $\mathcal{S}_U^+$

1. The integral representation (2.53) promotes us to separate  $\mathcal{S}^+$  into two regions. In the region  $\mathcal{S}_L^+$ ,  $u > v'$ , we may complete the integral contour from lower half plane. Since  $f(\omega, \gamma)$  contains QNMs in the lower half plane and branch cut along the negative imaginary axis [39], the contour is chosen as figure 3. This kind of contour is conventionally used, e.g., [46]. In this region, the Carrollian correlator  $C(u, \Omega; v', \Omega')$  receives contributions from the residues at the QNMs and the discontinuity while across the branch cut in the negative imaginary axis. On the other hand, in the region  $\mathcal{S}_U^+$ ,  $u < v'$ , we may complete the integral contour from upper half plane. The contour is chosen as figure 4. There are no QNMs in the upper half plane and the Carrollian correlator  $C(u, \Omega; v', \Omega')$  only receives contribution from the branch cut in the positive imaginary axis.
2. Similarly, the integral representation (2.57) motivates us to separate  $\mathcal{H}^+$  into another two regions. In the region  $\mathcal{H}_V^+$ ,  $v < v'$ , we may complete the integral contour from the upper half plane. Only branch cut may contribute to the integral. However, note that  $\mathcal{H}_U^+$  is located outside of the future light cone of  $v'$ , the retarded Green's function should be zero

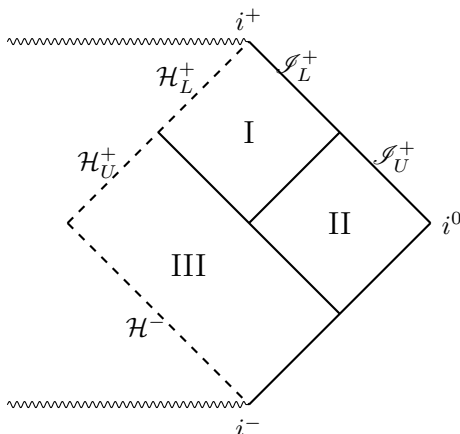


**Figure 5:** Classification of the asymptotically flat region  $\text{AFS}_1$  and its boundaries. The lightrays are emanating from  $v'$  in all directions, as well as a third ray which reflects from the black hole potential. These lightrays divide the asymptotically flat region  $\text{AFS}_1$  into three regions I, II, III. Furthermore, the ingoing lightray separates the event horizon  $\mathcal{H}^+$  into two regions  $\mathcal{H}_L^+$  and  $\mathcal{H}_U^+$ . The reflected lightray separates the future null infinity  $\mathcal{I}^+$  into another two regions  $\mathcal{I}_L^+$  and  $\mathcal{I}_U^+$ .

due to causality and thus

$$\tilde{C}(v, \Omega; v', \Omega') = 0, \quad v < v'. \quad (2.63)$$

On the other hand, in the region  $\mathcal{H}_L^+$ , we can complete the integral contour in the lower half plane. In this case, the contour is still chosen as in figure 3, both of the QNMs and the branch cut contribute to the Carrollian correlator  $\tilde{C}$ .

3. We have shown the regions  $\mathcal{I}_{U/L}^+, \mathcal{H}_{U/L}^+$  in figure 5 and extended them into the bulk. In the bulk, we find three regions I, II, III. Region I is connected to  $\mathcal{I}_L^+$  and  $\mathcal{H}_L^+$  and this region is related to the late time behaviour of the retarded Green's function. Region II is connected to  $\mathcal{I}_U^+$  and it is related to the early time behaviour of the retarded Green's function. Region III is connected to  $\mathcal{H}_U^+$  and  $\mathcal{H}^-$ , in which the retarded Green's function vanishes. The conclusion is consistent with the analysis in Schwarzschild-dS spacetime [47].

Before we close this subsection, we should mention that the reflection amplitude, a frequency space representation of the Carrollian amplitude from  $\mathcal{I}^-$  to  $\mathcal{I}^+$ , is determined by the formula (2.30), which closely mirrors the retarded Green's function of an AdS black hole [48]. It would be interesting to explore its relation to the flat space limit of an AdS black hole, following the approach of [49]. However, it seems that the flat space limit of the other Carrollian amplitude, from  $\mathcal{I}^-$  to  $\mathcal{H}^+$ , is absent in AdS/CFT. This topic certainly deserves further investigation.

## 2.3 Approximation of the Carrollian correlator

The reflection/transmission amplitude in black hole scattering is rather involved and thus it is not easy to obtain an analytic result for the Carrollian correlator. In Schwarzschild black hole, they are determined by the confluent Heun equation with boundary conditions of retarded Green's function. The problem is solved by mapping it to the a four-dimensional  $\mathcal{N} = 2$  supersymmetric gauge theory with three fundamental hypermultiplets [50]. The reflection and transmission amplitude are obtained by semiclassical Virasoro conformal blocks in the context of AGT correspondence [51, 52]. In this work, we will focus on several interesting properties of Carrollian correlator and leave a detailed analysis of the Carrollian correlator in a further study.

**Late time behaviour.** When  $u > v'$ , we should use the integration contour in figure 3. The residues at the QNMs lead to an exponential decay that is important in the ringdown phase. On the other hand, the branch cut along the negative frequency axis contributes to a power-law tail in the late time. More explicitly, for low frequencies,  $M\omega \ll 1$ , the solutions in the large  $r$  and near horizon are governed by hypergeometric function or its confluent version. By matching the two asymptotic solutions in the intermediate region, one finds [53]

$$A_{\omega,\ell}^{\text{in,up}} = (4iM\omega)^{-\ell-1} \left\{ 1 - \frac{1}{4} \left[ \frac{(\ell!)^3}{(2\ell)!(2\ell+1)!} \right]^2 (4\omega M)^{2\ell+2} + \dots \right\}, \quad (2.64a)$$

$$A_{\omega,\ell}^{\text{in,down}} = (-4iM\omega)^{-\ell-1} \left\{ 1 + \frac{1}{4} \left[ \frac{(\ell!)^3}{(2\ell)!(2\ell+1)!} \right]^2 (4\omega M)^{2\ell+2} + \dots \right\}. \quad (2.64b)$$

We note that for each mode with fixed  $\ell$ , the reflection amplitude is

$$(-1)^{\ell+1} \mathcal{R}_{\omega,\ell} = 1 + \frac{1}{2} \left[ \frac{(\ell!)^3}{(2\ell)!(2\ell+1)!} \right]^2 (4\omega M)^{2\ell+2} + \dots. \quad (2.65)$$

Integrating the integral along the branch cut leads to the power-law (from the  $\ell = 0$  modes)

$$C(u, \Omega; v', \Omega'^P) \propto \frac{1}{(u - v')^2} + \dots, \quad u \gg v'. \quad (2.66)$$

This is the Price's law at  $\mathcal{I}^+$  [54]. Note that the power-law tail is  $t^{-3}$  at timelike infinity [55]. This is the late time behavior of the Carrollian correlator since we just used the low frequency limit.

**Eikonal approximation.** A particularly tractable regime is the eikonal limit, where the energies are large and the momentum transfer is small. This eikonal approximation is known

as a method to sum over an infinite tower of Feynman diagrams in QFTs to describe the emergence of classical physics [56–59]. In gravitational physics, there is a nice correspondence between the ultra-relativistic  $2 \rightarrow 2$  scalar scattering and  $1 \rightarrow 1$  scattering in a shock wave spacetime [60, 61] and thus resummation of Feynman diagrams could reproduce the effect of classical geometries [62, 63]. This has been extended to the  $1 \rightarrow 1$  scattering amplitude in any stationary spacetime. More precisely, the  $1 \rightarrow 1$  massless scattering amplitude  $\mathcal{A}_2$  in a Schwarzschild spacetime is [64]

$$\mathcal{A}_2 = \frac{\pi}{2M} \delta(p^0 - p'^0) \mathcal{A}_{\text{eik}}(p, p') \quad (2.67)$$

where  $p^\mu, p'^\mu$  are the incoming and outgoing momenta of the scalar and  $M$  is the mass of the black hole. The so-called eikonal amplitude is

$$\mathcal{A}_{\text{eik}} = 8\pi \frac{\alpha(s)^2}{t} \frac{\Gamma(-i\alpha(s))}{\Gamma(i\alpha(s))} \left( \frac{4\mu^2}{-t} \right)^{-i\alpha(s)} \quad (2.68)$$

where  $s$  and  $t$  are Mandelstam invariants and  $\mu$  is an IR regulator. We denote the momentum of the background as  $P^\mu$  with

$$P^\mu = M(1, 0, 0, 0) \quad (2.69)$$

and the incoming and outgoing momenta are

$$p^\mu = \omega n^\mu = \omega(1, n^i), \quad p'^\mu = \omega' n'^\mu = \omega'(1, n'^i). \quad (2.70)$$

Here  $\omega, \omega'$  are energy of the incoming and outgoing massless scalars, respectively. Thus the Mandelstam invariants are

$$s = -(p + P)^2 = M^2 + 2M\omega, \quad t = -(p - p')^2 = 2\omega\omega' n \cdot n' = -4\omega\omega' \sin^2 \frac{\gamma}{2}. \quad (2.71)$$

Thus the function  $\alpha(s)$  is

$$\alpha(s) \equiv s - M^2 = 2\omega M \quad (2.72)$$

and the eikonal amplitude  $\mathcal{A}_{\text{eik}}$  is

$$\mathcal{A}_{\text{eik}} = -\frac{8\pi M^2 \omega}{\omega' \sin^2 \frac{\gamma}{2}} \frac{\Gamma(-2iM\omega)}{\Gamma(2iM\omega)} \left( \frac{\mu^2}{\omega\omega' \sin^2 \frac{\gamma}{2}} \right)^{-2iM\omega}. \quad (2.73)$$

The Carrollian amplitude is <sup>5</sup>

$$B(u, \Omega; v', \Omega') = \left( \frac{i}{8\pi^2} \right)^2 \int_0^\infty d\omega \int_0^\infty d\omega' e^{-i\omega' u + i\omega v'} \mathcal{A}_2$$

---

<sup>5</sup>The Carrollian amplitude considered here is slightly generalized because the background is a Schwarzschild black hole. From the perspective of  $2 \rightarrow 2$  scattering, two of the momenta are massive and describe the background, while the other two are massless. The Fourier transform in this Carrollian amplitude applies only to the massless particles, making it a partial Carrollian amplitude [65]. Further discussion on the celestial analog can be found in [66].

$$= \frac{M}{16\pi^2 \sin^2 \frac{\gamma}{2}} \int_0^\infty d\omega e^{-i\omega(u-v')} \frac{\Gamma(-2iM\omega)}{\Gamma(2iM\omega)} \left( \frac{\mu^2}{\omega^2 \sin^2 \frac{\gamma}{2}} \right)^{-2iM\omega}. \quad (2.74)$$

To relate it to the Carrollian correlator  $C(u, \Omega; v', \Omega')$  from  $\mathcal{S}^-$  to  $\mathcal{S}^+$ , we should extract the imaginary part

$$\begin{aligned} C(u, \Omega; v', \Omega') &= B(u, \Omega; v', \Omega') - B^*(u, \Omega; v', \Omega') \\ &= \frac{M}{16\pi^2 \sin^2 \frac{\gamma}{2}} \int_{-\infty+i\epsilon}^{\infty+i\epsilon} d\omega e^{-i\omega(u-v')} \frac{\Gamma(-2iM\omega)}{\Gamma(2iM\omega)} \left( \frac{\mu^2}{\omega^2 \sin^2 \frac{\gamma}{2}} \right)^{-2iM\omega} \\ &= \frac{1}{32\pi^2 \sin^2 \frac{\gamma}{2}} \int_{-\infty+i\epsilon}^{\infty+i\epsilon} dx e^{-ixz} \frac{\Gamma(-ix)}{\Gamma(ix)} (x^2)^{ix} \end{aligned} \quad (2.75)$$

where we have defined

$$z = \frac{u - v'}{2M} + 2 \ln \frac{2M\mu}{|\sin \frac{\gamma}{2}|}. \quad (2.76)$$

We have inserted  $i\epsilon$  in reference to the previous section. There is no analytic result for the integral<sup>6</sup>. However, one finds that the Carrollian correlator  $C(u, \Omega; v', \Omega')$  is a function of  $z$  up to a factor that is determined by the deflection angle

$$C(u, \Omega; v', \Omega') = \frac{1}{32\pi^2 \sin^2 \frac{\gamma}{2}} \mathcal{I}(z) \quad (2.77)$$

where

$$\mathcal{I}(z) = \int_{-\infty+i\epsilon}^{\infty+i\epsilon} dx e^{-ixz} \frac{\Gamma(-ix)}{\Gamma(ix)} (x^2)^{ix}. \quad (2.78)$$

As a function of a complex variable  $z$ , The poles and branch cuts of  $\mathcal{I}(z)$  should reflect the physical properties of the Carrollian correlator  $C(u, \Omega; v', \Omega')$ . Indeed, when  $z > 0$ , we may choose the contour in the lower half plane to evaluate the integral. On the other hand, when  $z < 0$ , we may choose the contour in the upper half plane to evaluate the integral. Therefore,  $z = 0$  determines a constraining equation between the incoming and outgoing data

$$\frac{u - v'}{2M} + 2 \ln \frac{2M\mu}{|\sin \frac{\gamma}{2}|} = 0. \quad (2.79)$$

Physically, a classical massless particle coming from  $(v', \Omega') \in \mathcal{S}^-$  propagates along a null geodesic and arrives at  $(u, \Omega) \in \mathcal{S}^+$ . This already determines a classical equation between the initial and final data via the null geodesic. To check this point, we notice that the deflection angle is small in the eikonal approximation and thus the equation is approximately

$$u - v' + 4M \ln \frac{4M\mu}{\gamma} = 0. \quad (2.80)$$

---

<sup>6</sup>However, the integral can be evaluated order by order by expanding the last term  $x^{-2ix}$ . And the first term corresponds to the contribution of the Newton potential. Please find more details in appendix A.

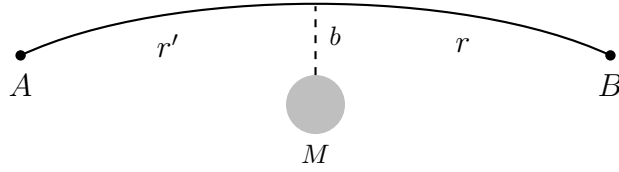


**Figure 6:** Shapiro delay. A light is deflected by the massive object with mass  $M$ . The distance between  $A/B$  and  $M$  is  $r'/r$  and the turning point to  $M$  is approximately equal to the impact parameter  $b$ .

The deflection angle of the light is

$$\gamma = \frac{4M}{b} \quad (2.81)$$

where  $b$  is the impact parameter and thus

$$u - v' + 4M \ln \mu b = 0. \quad (2.82)$$

We introduce two IR regulators  $r \gg 2M$  and  $r' \gg 2M$  and thus

$$(t - r_*(r)) - (t' + r_*(r')) + 4M \ln \mu b = 0 \quad \Rightarrow \quad t - t' - (r + r') \approx 2M \ln \frac{rr'}{4M^2 \mu^2 b^2}. \quad (2.83)$$

In flat spacetime,  $r + r'$  is the duration for a light that is emitted from the initial point and received in the final point. Thus the left hand side is the Shapiro time delay during the process

$$(\Delta t)_{\text{shapiro}} \approx 2M \ln \frac{rr'}{4M^2 \mu^2 b^2}. \quad (2.84)$$

Figure 6 is a schematic diagram for the Shapiro delay. A light is emitted from A and reflected from B and finally received by A, the Shapiro delay is [67]

$$(\Delta t)_{A \rightarrow B \rightarrow A} = 4M \left( 1 + \ln \frac{4rr'}{b^2} \right). \quad (2.85)$$

To match the logarithm between (2.84) and (2.85), we should identify the IR regulator  $\mu$  from the scattering amplitude with <sup>7</sup>

$$1 + 4 \ln 2 + 2 \ln M\mu = 0. \quad (2.86)$$

Note that (2.85) should divide a factor 2 to match with (2.84) since the time delay in (2.84) is for a single travel.

<sup>7</sup>In the following section, we will find a more precise relation between  $\mu$  and the reference point in the definition of tortoise coordinate.

### 3 Classical equations at null boundaries

In the previous section, we clarified the relationship between the Carrollian correlators and the reflection and transmission amplitudes in black hole  $1 \rightarrow 1$  scattering. The reflection and transmission amplitudes are defined via the partial wave expansion and the poles in these amplitudes are called QNMs. On the other hand, the Carrollian correlators are the dual descriptions of the same process. Physically, there should be poles for the Carrollian correlators in the position space. According to the propagation theorem of singularity [68, 69], the poles should be determined by the null geodesics coming from  $\mathcal{I}^-$ <sup>8</sup>. More precisely, the geodesics from  $\mathcal{I}^-$  to  $\mathcal{I}^+$  define a classical equation

$$\mathcal{F}(u, \Omega; v', \Omega') = 0. \quad (3.1)$$

Similarly, the poles of the Carrollian correlator  $\tilde{C}(v, \Omega; v', \Omega')$  should be governed by the null geodesics from  $\mathcal{I}^-$  to  $\mathcal{H}^+$  and thus define another equation

$$\tilde{\mathcal{F}}(v, \Omega; v', \Omega') = 0. \quad (3.2)$$

Depending on the impact parameter, the equation (3.1) exists for  $b > b_c$  while (3.2) exists for  $b < b_c$ . The critical value  $b_c = 3\sqrt{3}M$  is determined by the impact parameter of the photon sphere. In the following, we will derive the two equations and discuss their properties.

#### 3.1 From $\mathcal{I}^-$ to $\mathcal{I}^+$

The null geodesics are shown in figure 7. It starts from  $(v', \Omega')$ , passes through the turning point  $(t_0, r_0, \Omega_0)$  and arrives at  $(u, \Omega)$ . For the first part of the journey, we use the ingoing Eddington-Finkelstein coordinates  $(v, r, \Omega)$  such that the metric is

$$ds^2 = -Adv^2 + 2dvdr + r^2d\Omega. \quad (3.3)$$

We fix the geodesics in the equatorial plane  $\theta = \theta_0 = \theta' = \frac{\pi}{2}$  using spherical symmetry. Due to the time translation invariance and the rotational symmetry of the metric, we may assume the Hamilton-Jacobi action as

$$S = -Ev + R(r; E, L) + L\phi \quad (3.4)$$

where  $E$  and  $L$  are the energy and angular momentum of the light. The action  $S$  obeys the eikonal equation

$$g^{\mu\nu} \partial_\mu S \partial_\nu S = 0. \quad (3.5)$$

---

<sup>8</sup>Roughly speaking, this states that singularities propagate along null geodesics. This property can also be found by the Hadamard form for the retarded Green function [70]. We should mention that Hadamard form is valid only in convex geodesic domains. More discussion on the singularity structure of the Green's function can be found in [71, 72].

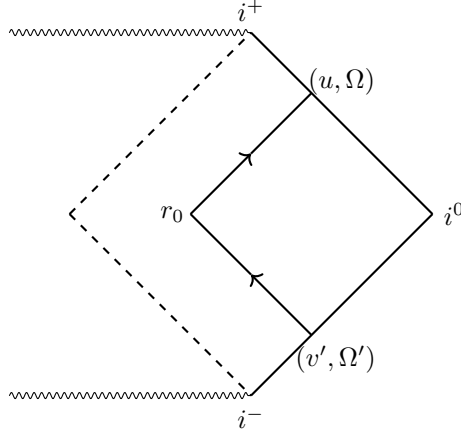


**Figure 7:** Deflection of light in Schwarzschild spacetime.

A constant  $S$  defines a hypersurface in the spacetime whose co-normal vector is the momentum 1-form

$$p_\mu = \frac{\partial S}{\partial x^\mu}. \quad (3.6)$$

To be more precise,

$$p_0 = -E, \quad p_\phi = L, \quad p_r = \frac{\partial R(r; E, L)}{\partial r}. \quad (3.7)$$

Substituting into the equation (3.5), we find

$$p_r = \frac{E}{A} \left( 1 - \sqrt{1 - A \frac{b^2}{r^2}} \right). \quad (3.8)$$

Since  $S$  is a constant along the geodesics, we find

$$v = \frac{\partial R}{\partial E} \Big|_L, \quad \phi = -\frac{\partial R}{\partial L} \Big|_E. \quad (3.9)$$

Thus, we find the relation of the coordinates along the geodesics

$$v_0 - v' = v(r_0) - v(r \rightarrow \infty) = \int_\infty^{r_0} dr \frac{\partial p_r}{\partial E} \Big|_L = \int_{r_0}^\infty dr \frac{1 - \sqrt{1 - \frac{Ab^2}{r^2}}}{A \sqrt{1 - \frac{Ab^2}{r^2}}}, \quad (3.10a)$$

$$\phi_0 - \phi' = \phi(r_0) - \phi(r \rightarrow \infty) = - \int_\infty^{r_0} dr \frac{\partial p_r}{\partial L} \Big|_E = \int_{r_0}^\infty dr \frac{1}{r \sqrt{\frac{r^2}{b^2} - A}}. \quad (3.10b)$$

One can derive the same result using Killing vectors and solve the geodesic equations. The turning point  $r_0$  is determined by the largest positive root of the equation

$$r_0^2 = A(r_0)b^2. \quad (3.11)$$

The photon sphere corresponds to  $r_0 = r_{ps} = 3M$  and  $b = b_c = 3\sqrt{3}M$ . For  $b > b_c$ , we find

$$v_0 - v' = \int_{r_0}^{\infty} dr \frac{1 - \sqrt{1 - \frac{A(r)r_0^2}{r^2 A(r_0)}}}{A(r) \sqrt{1 - \frac{A(r)r_0^2}{r^2 A(r_0)}}}, \quad (3.12a)$$

$$\phi_0 - \phi' = \int_{r_0}^{\infty} dr \frac{1}{r \sqrt{\frac{r^2}{r_0^2} A(r_0) - A(r)}}. \quad (3.12b)$$

The equations (3.12) defines an equation between  $v_0 - v'$  and  $\phi_0 - \phi'$  since both of them are parameterized by  $r_0 > 3M$ .

For the outgoing trip, we switch to the outgoing Eddington-Finkelstein coordinates  $(u, r, \Omega)$  and find a set of similar equation

$$u - u_0 = \int_{r_0}^{\infty} dr \frac{1 - \sqrt{1 - \frac{A(r)r_0^2}{r^2 A(r_0)}}}{A(r) \sqrt{1 - \frac{A(r)r_0^2}{r^2 A(r_0)}}}, \quad (3.13a)$$

$$\phi - \phi_0 = \int_{r_0}^{\infty} dr \frac{1}{r \sqrt{\frac{r^2}{r_0^2} A(r_0) - A(r)}}. \quad (3.13b)$$

The coordinates at the turning point should be eliminated. Therefore, we should glue the two sets of equations (3.12) and (3.13) at  $r_0$  to get

$$u - v' = 2 \int_{r_0}^{\infty} dr \frac{1 - \sqrt{1 - \frac{A(r)r_0^2}{r^2 A(r_0)}}}{A(r) \sqrt{1 - \frac{A(r)r_0^2}{r^2 A(r_0)}}} - 2r_*(r_0), \quad (3.14a)$$

$$\phi - \phi' = 2 \int_{r_0}^{\infty} dr \frac{1}{r \sqrt{\frac{r^2}{r_0^2} A(r_0) - A(r)}}. \quad (3.14b)$$

We have used the relation

$$u_0 - v_0 = -2r_*(r_0) \quad (3.15)$$

at the turning point. We may eliminate  $r_0$  and get the equation

$$\frac{u - v'}{M} = h(\gamma) \quad (3.16)$$

where  $\gamma = \phi - \phi' - \pi$  is the deflection angle. The above equation is the implicit form of the equation (3.1). Figure 8 is the curve for the equation that connects the deflection angle and the time delay<sup>9</sup>. Properties are discussed in the following:

---

<sup>9</sup>Strictly speaking, there is a small region that  $u - v'$  is negative and it is not suitable to use the word

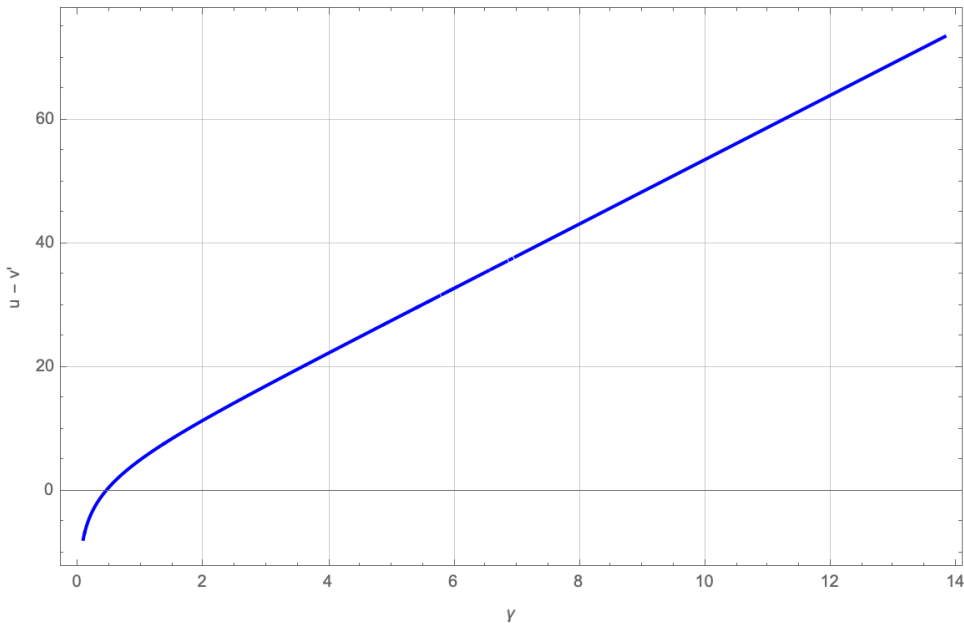


**Figure 8:** The equation  $u - v' = h(\gamma)$  that connects the deflection angle and the time delay for  $b > b_c$ . We have set  $M = 1$  in the diagram.

1. Note that the deflection angle  $\gamma$  can exceed  $\pi$  in the figure. In principle, the azimuthal angle is periodic which leads to the identification

$$\gamma \sim \gamma + 2\pi. \quad (3.17)$$

However, the integration (3.14b) ignores this fact and it has the advantage to encode the winding number for the light to wrap around the black hole. For example, when  $b \rightarrow b_c$ , an incoming light should wrap around the black hole multiple times before it escapes from the gravitational potential. Due to this reason, we have extended the domain of deflection angle. The winding number is the integer part of  $\frac{\gamma}{2\pi}$

$$w = \lfloor \frac{\gamma}{2\pi} \rfloor. \quad (3.18)$$

Now the time delay  $u - v'$  is a monotonically increasing function of  $\gamma$ .

2. When the deflection angle  $\gamma \rightarrow 0$ , the impact parameter is large and we find the logarithm behavior

$$\frac{u - v'}{M} = 4 \ln \gamma + 2 + 4\zeta + 4 \ln(\zeta - 1), \quad \gamma \rightarrow 0. \quad (3.19)$$

---

“delay”. Also, the equation (3.16) is not exactly the same meaning as Shapiro delay. In Shapiro delay, the time delay  $t - t'$  is related to the impact parameter. However, in our equation, the time delay  $u - v'$  is related to the deflection angle. It should be understood as a consequence of the combination of the light deflection and Shapiro delay.

This result matches with (2.80) by connecting the IR regulator  $\mu$  with the choice of the reference point  $o$  via

$$1 + 2\zeta + 2 \ln(\zeta - 1) + 2 \ln 4M\mu = 0. \quad (3.20)$$

With the standard reference point, we find

$$\frac{u - v'}{M} = 4 \ln \gamma + 2 + \mathcal{O}(\gamma^{-1}). \quad (3.21)$$

We have proved the logarithmic behavior in appendix B. Note that this region corresponds to the weak field limit, the difference  $u - v' < 0$  and the outgoing light arrives at  $\mathcal{S}_U^+$ . The critical point  $u - v' = 0$  depends on the reference point. For the standard choice of  $o$ , we find the critical deflection angle

$$\gamma_0 \approx 0.4352. \quad (3.22)$$

The corresponding impact parameter and the turning point are

$$b_0 = 12.3455, \quad r_0 = 11.1877. \quad (3.23)$$

- When  $\gamma \gg 1$ , the time delay  $u - v'$  is a linear function of  $\gamma$ . This is in the strong field region. In appendix B, we have proved that

$$\frac{u - v'}{M} = 3\sqrt{3}\gamma + c_0 + \mathcal{O}(\gamma^{-1}) \quad (3.24)$$

in the large  $\gamma$  limit and the constant  $c_0$  can be found in (B.44). The slope of the curve  $3\sqrt{3}$  is actually equal to the impact parameter  $b_c$ . Physically, when  $b \rightarrow b_c$ , the light wraps around the photon sphere and the main contribution of the time delay is from the winding around the photon sphere. The angular frequency of the photon around the photon sphere is

$$\Omega_c = \left. \frac{d\phi}{dt} \right|_{r=r_{ps}} = \frac{1}{b_c}. \quad (3.25)$$

Therefore, the time delay is approximately equal to the product of winding number and  $b_c$ . This interprets the linear function (3.24) in the large  $\gamma$  limit. Given a deflection angle  $\gamma \in (0, \pi)$ , then from the figure one finds that  $\gamma + 2\pi w$ ,  $w \geq 1$  is already large and the linear approximation is valid. Consider a light ray emitting near  $\mathcal{S}^-$  with fixed  $(v', \Omega')$  and a detector that is located near  $\mathcal{S}^+$  at a fixed angle  $\Omega$ , as shown in figure 9, the light ray may wrap around the photon sphere many times to arrive at the detector. Then the observer will detect signals at equal time intervals<sup>10</sup>

$$h(\gamma + 2\pi(w + 1)) - h(\gamma + 2\pi w) \approx 2\pi b_c \quad (3.26)$$

---

<sup>10</sup>In fact, there are light rays that orbit the black hole in the opposite direction, whose corresponding deflection angle is  $2\pi - \gamma$ . For an observer at a fixed angle near  $\mathcal{S}^+$ , the signals are received alternately, first from one direction and then the other.

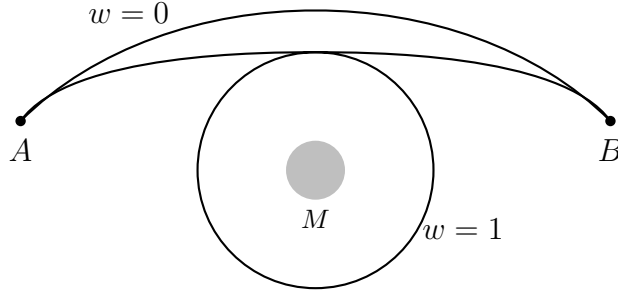


**Figure 9:** Light rays with different winding numbers ( $w = 0, 1$ ) emitted from A and received at B.

for any positive winding number  $w \geq 1$ . The exception case is  $w = 0$  where  $h(\gamma)$  may not be a linear function of  $\gamma$  once the deflection angle is small.

4. Comparison with the results in the literature. In [73], the logarithmic divergence for the deflection angle  $\gamma = -\ln\left(\frac{b}{b_c} - 1\right)$  has been derived in the strong field region. Then our results show a similar logarithmic divergence for the time delay in the same region

$$u - v' = -3\sqrt{3}M \ln\left(\frac{b}{b_c} - 1\right). \quad (3.27)$$

This is consistent with [74].

5. Relationship between time delay and deflection angle of neighboring light rays. For neighboring light rays emitted from the same position  $(v', \Omega')$  with slightly different impact parameters, their deflection angles and time delays are also slightly different. The relation is governed by the derivative

$$\frac{d(u - v')}{d\gamma} = Mh'(\gamma). \quad (3.28)$$

The asymptotic behavior of  $h'(\gamma)$  is

$$h'(\gamma) = \begin{cases} \frac{4}{\gamma} + \dots, & \gamma \rightarrow 0, \\ 3\sqrt{3} + \dots, & \gamma \rightarrow \infty. \end{cases} \quad (3.29)$$

The strong-field limit result is consistent with that in [75].

6. We may use an analytic function  $g(\gamma)$  to fit the curve  $h(\gamma)$

$$g(\gamma) = \alpha_1 \ln(e^{\alpha_2 \gamma} - 1) + \alpha_3 \ln(e^{\alpha_4 \gamma} - 1) + \alpha_5 \quad (3.30)$$

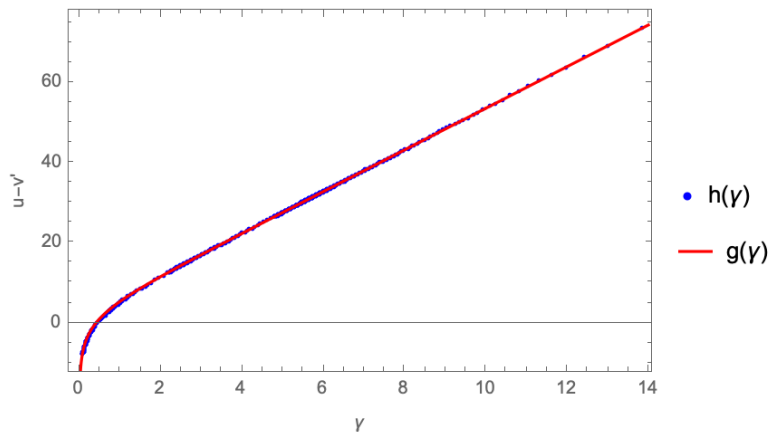


**Figure 10:** We fit the curve  $h(\gamma)$  using the function  $g(\gamma)$  by setting  $\alpha_1 = 0.738$ ,  $\alpha_2 = 0.615$ ,  $\alpha_3 = 3.262$ ,  $\alpha_4 = 1.454$ ,  $\alpha_5 = 1.674$ .

where  $\alpha_i$ ,  $i = 1, 2, \dots, 5$  are constants. By assuming  $\alpha_2, \alpha_4 > 0$  and matching with  $h(\gamma)$  in the small and large  $\gamma$  limit, we find four equations for  $\alpha_i$ 's

$$\alpha_1 \ln \alpha_2 + \alpha_3 \ln \alpha_4 + \alpha_5 = 2, \quad (3.31a)$$

$$\alpha_1 + \alpha_3 = 4, \quad (3.31b)$$

$$\alpha_1 \alpha_2 + \alpha_3 \alpha_4 = 3\sqrt{3}, \quad (3.31c)$$

$$\alpha_5 = c_0. \quad (3.31d)$$

This does not fix all the constants uniquely; we can adjust the values to fit the curve  $h(\gamma)$ . Figure 10 shows a function  $g(\gamma)$  that fits  $h(\gamma)$ . The function  $g(\gamma)$  matches  $h(\gamma)$  nicely over the whole region. However, it should be noted that in the intermediate region (e.g.,  $0.2 < \gamma < 0.8$ ), the differences between the two functions are smoothed out due to the large scale of the figure. In figure 11, we zoom into the intermediate region and see that small differences indeed exist.

7. The previous properties can be extended to general spherically symmetric spacetimes. Further details can be found in appendix B.

### 3.2 From $\mathcal{I}^-$ to $\mathcal{H}^+$

The discussion in the previous subsection should be modified when  $0 \leq b < b_c$ . In this case, a light ray from  $\mathcal{I}^-$  will cross the potential carrier and arrive at  $\mathcal{H}^+$ . This is shown in figure 12. The time delay is  $v - v'$  and the deflection angle is  $\gamma = \phi - \phi'^{11}$

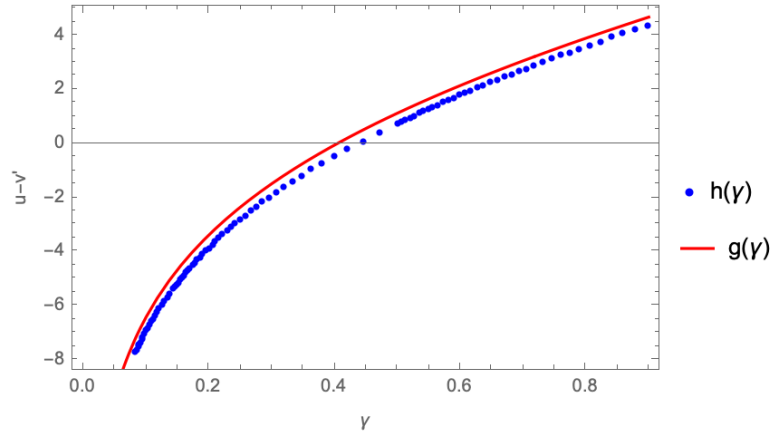


**Figure 11:** The functions  $h(\gamma)$  and  $g(\gamma)$  in the intermediate region  $0.1 < \gamma < 0.9$ .

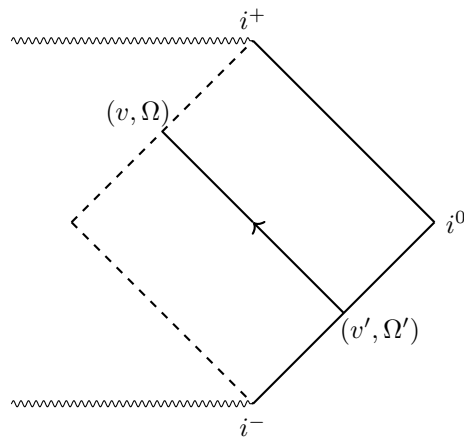


**Figure 12:** The geodesics that falls into the Schwarzschild black hole.

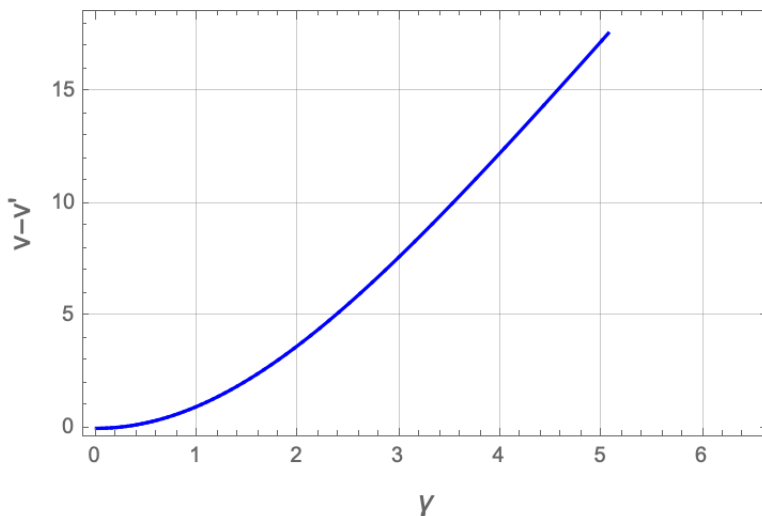


**Figure 13:** The equation  $v - v' = H(\gamma)$  that connects the deflection angle and the time delay for  $b < b_c$ . We have set  $M = 1$  in the diagram.

$$v - v' = \int_{r_h}^{\infty} dr \frac{1 - \sqrt{1 - \frac{A(r)b^2}{r^2}}}{A(r)\sqrt{1 - \frac{A(r)b^2}{r^2}}}, \quad (3.32a)$$

$$\phi - \phi' = \int_{r_h}^{\infty} dr \frac{1}{r\sqrt{\frac{r^2}{b^2} - A(r)}} \quad (3.32b)$$

where  $r_h = 2M$  is the Schwarzschild radius. The functions (3.32) are parameterized by the impact parameter  $0 \leq b < b_c$  and we write the function (3.2) as follows:

$$v - v' = H(\gamma). \quad (3.33)$$

Figure 13 is the function  $H(\gamma)$ . Similar to  $h(\gamma)$ , it is also a monotonically increasing function of  $\gamma$  but with a completely different behaviour.

1. The time delay  $v - v'$  is always non-negative

$$v - v' \geq 0. \quad (3.34)$$

This is consistent with the Carrollian correlator from  $\mathcal{I}^-$  to  $\mathcal{H}^+$  since it is non-vanishing only for  $v > v'$

$$\tilde{C}(v, \Omega; v', \Omega') \propto \Theta(v - v'). \quad (3.35)$$

When  $v < v'$ , no light can propagate to  $\mathcal{H}^+$  as this scenario breaks causality.

---

<sup>11</sup>Note that the definition of the deflection angle is not the same as the previous subsection. We will not subtract  $\pi$  from  $\phi - \phi'$  which ensures that  $\gamma$  is always greater than zero.

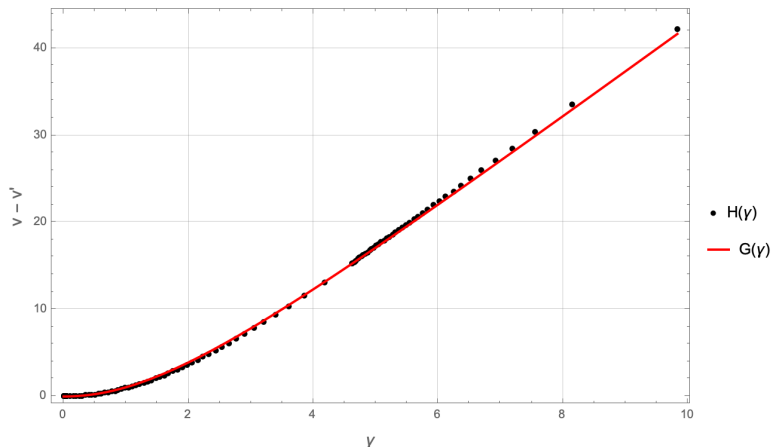


**Figure 14:** We fit the curve  $H(\gamma)$  using the rational function  $G(\gamma)$ .

2. When the impact parameter  $b \rightarrow 0$ , the light plunges into the black hole directly. This corresponds to the small deflection angle limit  $\gamma \rightarrow 0$ , and find a hyperbola behaviour

$$\frac{v - v'}{M} = \gamma^2 + \mathcal{O}(\gamma^4). \quad (3.36)$$

This is proven in appendix C.

3. When the impact parameter  $b \rightarrow b_c^-$ , the light circles around the photon sphere many times before it falls into the black hole. This corresponds to the limit  $\gamma \rightarrow \infty$ , and we find a linear behaviour

$$\frac{v - v'}{M} = 3\sqrt{3}\gamma + \tilde{c}_0 + \mathcal{O}(\gamma^{-1}). \quad (3.37)$$

This is discussed in appendix C.

4. We can use a rational function

$$G(\gamma) = \frac{a\gamma^2 + 3\sqrt{3}\gamma^3}{\frac{2a\gamma}{3\sqrt{3}} + a + \gamma^2}, \quad a = -\tilde{c}_0 = 8.878 \quad (3.38)$$

to fit the function  $H(\gamma)$ . One can check that  $G(\gamma)$  and  $H(\gamma)$  have the same asymptotic expansion for  $\gamma \rightarrow \infty$  and  $\gamma \rightarrow 0$ . Figure 14 shows that the difference of these two functions is small.

## 4 Conclusion and discussion

In this work, we derive two-point Carrollian correlators in Schwarzschild black hole perturbation theory. The regularized correlator from  $\mathcal{I}^-$  to  $\mathcal{I}^+$  is the Fourier transform of the

scattering amplitude in a partial wave expansion and is free of IR divergence. By contrast, the correlator from  $\mathcal{I}^-$  to  $\mathcal{H}^+$  has not been discussed in previous works. These two correlators are determined by the reflection and transmission amplitudes, respectively. We focus on the poles of the correlators, which are determined by the light rays connecting the initial and final null boundaries. These poles are encoded in two equations that determine the relationship between Shapiro time delay and deflection angle. We analyze the asymptotic behavior of the equations in the limits of large and small deflection angles. The corresponding functions are monotonically increasing curves and can be fitted by simple analytic functions. Furthermore, the linear growth at large deflection angles is controlled by the photon sphere and thus reflects strong-field information. Many topics deserve further study:

- **Poles and reconstruction of Carrollian correlator.** It is well known that the null geodesics in Schwarzschild and even in Kerr spacetime are governed by elliptic functions [76]. Applications of elliptic functions in black hole physics can be found in [77]. In this work, the poles of the Carrollian correlators are parameterized by the impact parameter or the turning point. One should eliminate these parameters to obtain an analytic expression for the poles. It would be interesting to explore whether it is possible to reconstruct the Carrollian correlator from the knowledge of the poles. Such an approach may provide an alternative way to understand the QNMs [78] and the branch cuts of the Green's function in momentum space. QNMs have been studied for decades using various methods [79–85] and are also important for black hole spectroscopy [86]. Note that the geometric interpretations of the QNMs have already been discussed in [87,88]. It would be interesting to explore this topic from a Carrollian perspective.
- **Time domain behavior and angular distribution of Carrollian correlators.** The Carrollian correlator provides a position-space representation of the  $S$ -matrix, whereas the conventional scattering amplitude is typically developed in momentum space. The latter framework is adapted to particle physics and has found interesting applications in gravitational physics, as mentioned in the introduction. In contrast, the Carrollian correlator is the natural quantity to describe the wave aspects of objects. Indeed, in gravitational physics, one is primarily interested in the time domain behavior of gravitational waves and the angular distribution of the signals. Therefore, the Carrollian correlator serves as an ideal framework for understanding gravitational phenomena. In particular, for the Carrollian correlator  $C(u, \Omega; v', \Omega')$ , one expects a prompt transport at early times, an exponentially decaying ringdown phase at intermediate times, and a power-law tail at late times [89].
- **Ambiguity.** We have used Bondi coordinates to derive the Carrollian correlators and classical equations that characterize the relationship between the time delay and the deflection angle of light. An ambiguity arises from the choice of the reference point  $o$  corresponding to the definition of the tortoise coordinates. In (3.20), we could relate the

reference point to the IR regulator  $\mu$  in the scattering amplitude. The Bondi coordinate system is motivated by the need to adapt to asymptotic inertial observers, e.g., GW detectors. This is crucial because gravitational waveforms are always studied in a specific coordinate system. However, it should be emphasized that the choice of coordinates is one of the most delicate and, sometimes, confusing aspects of general relativity. Besides the previous ambiguity, there is an additional ambiguity from supertranslations. A supertranslation corresponds to an angle-dependent choice of the origin of the time coordinate. In terms of Bondi coordinates, this is the nontrivial transformation that preserves the asymptotic structure near  $\mathcal{I}^+$ ,

$$\tilde{u} = u + T(\Omega) + \mathcal{O}(r^{-1}), \quad \tilde{r} = r + \mathcal{O}(1), \quad \tilde{\theta}^A = \theta^A + \mathcal{O}(r^{-1}), \quad (4.1)$$

where  $T(\Omega)$  is a smooth function on  $S^2$  that parameterizes the supertranslation.<sup>12</sup> Note that there is a corresponding supertranslation near  $\mathcal{I}^-$ ,

$$\tilde{v} = v + T^{(-)}(\Omega) + \mathcal{O}(r^{-1}), \quad \tilde{r} = r + \mathcal{O}(1), \quad \tilde{\theta}^A = \theta^A + \mathcal{O}(r^{-1}). \quad (4.2)$$

It is claimed that the functions  $T^{(-)}$  and  $T$  are related via an antipodal map [96] such that there is a unique BMS transformation in the whole spacetime. Now the poles of the Carrollian correlator  $u - v' = h(\gamma)$  are sensitive to supertranslations.<sup>13</sup> This sensitivity suggests that the poles of the Carrollian correlator may be used to determine the BMS frame.

- **Kerr black hole.** Kerr spacetime is important for understanding various phenomena in astronomy [97]. Interestingly, the method presented in this work can be extended directly to Kerr spacetime. Several topics in this direction are worth exploring. First, in a rotating background, geodesics are not always confined to the equatorial plane. The constraint equations that describe the poles of the Carrollian correlator should include the polar angle. Moreover, there are various orbits in Kerr spacetime, depending on the initial data [98]. It would be interesting to explore how to understand these aspects from a Carrollian approach. Second, in Kerr spacetime, the scattering of radiation produces waves with an amplitude larger than that of the incident wave under certain conditions. This phenomenon is called superradiance [99–101] and is absent in Schwarzschild spacetime. Note that in the spherically symmetric case, the reflection amplitude is related to the Carrollian correlator via

$$(-1)^{\ell+1} \mathcal{R}_{\omega, \ell} = 1 - 4\pi \int_{-\infty}^{\infty} du \omega e^{i\omega u} \int_0^\pi \sin \gamma d\gamma C(u, \Omega; 0, \Omega^P) P_\ell(\cos \gamma). \quad (4.3)$$

---

<sup>12</sup>Choosing a function  $T(\Omega)$  means fixing a BMS frame. For each solution of general relativity, there is a supertranslated solution [90–92]. This BMS frame-fixing problem is also important in numerical relativity [93–95].

<sup>13</sup>Note that this is in contrast with the one in flat spacetime, where the pole equation reduces to  $u = v'$ ,  $\Omega = \Omega^P$ , and this equation is invariant upon imposing the antipodal map.

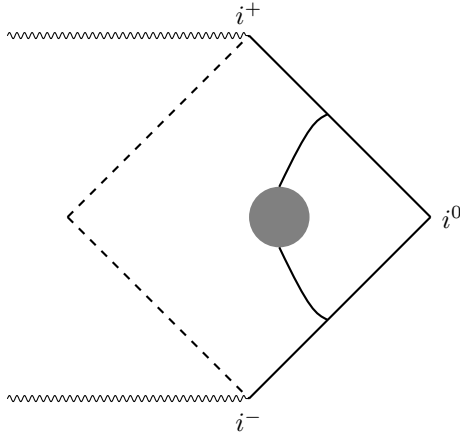


**Figure 15:** Higher-order corrections.

The absence of superradiance imposes constraints on the Carrollian correlator:

$$|\mathcal{R}_{\omega,\ell}|^2 \leq 1. \quad (4.4)$$

For a rotating spacetime, this inequality can be violated, and the constraints on the Carrollian correlator should be relaxed. It would be interesting to explore this point in the future.

- **Non-linear corrections.** In this work, we have studied the Carrollian correlator in black hole perturbation theory at the linearized level. From the perspective of scattering amplitudes, there are various non-linear corrections that can be written down systematically via Feynman rules, as shown in figure 15. Note that one should extract the classical aspects from the loop corrections. It would be interesting to explore their relation to second-order perturbation theory [102, 103] and the self-force problem [70, 104].

**Acknowledgments.** The work of J.L. is supported by NSFC Grant No. 12575074.

## A Integration

In this appendix, we will explore the relation between the integral  $\mathcal{I}(z)$  and the effect of Newton potential. We expand  $x^{2ix}$  as

$$x^{2ix} = \sum_{k=0}^{\infty} \frac{1}{k!} (2ix \ln x)^k \quad (A.1)$$

and then we can write  $\mathcal{I}(z)$  as a formal expansion

$$\mathcal{I}(z) = \sum_{k=0}^{\infty} \mathcal{I}_k(z) \quad (\text{A.2})$$

where the  $\mathcal{I}_0$  is

$$\mathcal{I}_0(z) = \int_{-\infty+i\epsilon}^{\infty+i\epsilon} dx e^{-izx} \frac{\Gamma(-ix)}{\Gamma(ix)}. \quad (\text{A.3})$$

This is non-vanishing only for  $z > 0$

$$\begin{aligned} \mathcal{I}_0(z) &= \Theta(z) \int_{-\infty+i\epsilon}^{\infty+i\epsilon} dx e^{-izx} \frac{\Gamma(-ix)}{\Gamma(ix)} \\ &= -2\pi i \Theta(z) \sum_{n=1}^{\infty} \text{Res}_{x=-in} \left( e^{-izx} \frac{\Gamma(-ix)}{\Gamma(ix)} \right) \\ &= 2\pi e^{-z} J_1(e^{-z}). \end{aligned} \quad (\text{A.4})$$

We have used residue theorem to find the integration. The Bessel function  $J_1(e^{-z})$  is real and non-negative for  $z > 0$ . Now we show that the same structure appears in the Carrollian correlator contributed by Newton potential.

In the geometric optics limit, one can use the WKB approximation to derive the phase shift factor [105, 106]. The starting point is the massless scattering problem in Schwarzschild space-time

$$\frac{d^2}{dr_*^2} G_{\ell,\omega}(r) + Q G_{\ell,\omega}(r) = 0 \quad (\text{A.5})$$

where  $Q = \omega^2 - V_{\ell}(r)$ . The lowest order WKB solution of this equation is

$$G_{\ell,\omega}(r) = Q^{-1/4} e^{i \int^r dr_* \sqrt{Q}} \propto e^{i S_r} \quad (\text{A.6})$$

where the phase  $S_r$  satisfies the Hamilton-Jacobi equation for a light ray with energy  $E = \omega$  and angular momentum  $L \approx \ell + \frac{1}{2}$ .

$$\left( \frac{dS_r}{dr} \right)^2 = \frac{1}{\Delta^2} (E^2 r^4 - L^2 \Delta) \quad \Rightarrow \quad \frac{dS_r}{dr} = \pm \frac{E}{A(r)} \sqrt{1 - \frac{A(r)b^2}{r^2}} \quad (\text{A.7})$$

where  $\Delta = r^2 - 2Mr = r^2 A(r)$  and the impact parameter  $b = \frac{|L|}{E}$ . To match the solution with the boundary condition at  $r_* \rightarrow \infty$ , the phase shift factor should be identified as [107]

$$\delta_{\ell} \approx \int_{r_0}^{\infty} dr \frac{1}{A(r)} (Q^{1/2} - E) - E r_*(r_0) + \frac{\pi}{2} L. \quad (\text{A.8})$$

We would expect that for the large  $L$  partial waves, it feels only the far-zone Newtonian field. In calculating the partial-wave sum for the scattering amplitude, it is convenient to split it into two terms

$$f(\omega, \gamma) = f_d(\omega, \gamma) + f_n(\omega, \gamma) \quad (\text{A.9})$$

where  $f_d$  represents the part of the scattering amplitude that carries the information of the main diffraction effects<sup>14</sup> while  $f_n$  denotes the amplitude coming from the Newton potential. The phase shift from the Newton potential has been solved explicitly by [110]

$$e^{2i\delta_\ell} = \frac{\Gamma(\ell + 1 - 2iM\omega)}{\Gamma(\ell + 1 + 2iM\omega)} \quad (\text{A.10})$$

and thus we have

$$f_n(\omega, \gamma) = M \frac{\Gamma(1 - 2iM\omega)}{\Gamma(1 + 2iM\omega)} \left( \sin^2 \frac{\gamma}{2} \right)^{-1+2iM\omega}. \quad (\text{A.11})$$

We can also decompose the boundary-to-boundary correlator into a Newtonian and a diffraction part

$$C(u, \Omega; v', \Omega') = C_n(u, \Omega; v', \Omega') + C_d(u, \Omega; v', \Omega') \quad (\text{A.12})$$

where contribution from the Newton potential is

$$\begin{aligned} C_n(u, \Omega; v', \Omega'^P) &\propto \int_{-\infty+i\epsilon}^{\infty+i\epsilon} d\omega f_n(\omega, \gamma) \\ &= M \int_{-\infty+i\epsilon}^{\infty+i\epsilon} d\omega e^{-i\omega(u-v')} \frac{\Gamma(1 - 2iM\omega)}{\Gamma(1 + 2iM\omega)} \left( \sin^2 \frac{\gamma}{2} \right)^{-1+2iM\omega} \\ &= -\frac{1}{2 \sin^2 \frac{\gamma}{2}} \int_{-\infty+i\epsilon}^{\infty+i\epsilon} dx e^{-ix \frac{u-v'}{2M}} \frac{\Gamma(-ix)}{\Gamma(ix)} e^{ix \ln \sin^2 \frac{\gamma}{2}} \\ &= -\frac{1}{2 \sin^2 \frac{\gamma}{2}} \int_{-\infty+i\epsilon}^{\infty+i\epsilon} dx e^{-i(\frac{u-v'}{2M} - 2 \ln |\sin \frac{\gamma}{2}|)x} \frac{\Gamma(-ix)}{\Gamma(ix)} \\ &\propto \frac{1}{\sin^2 \frac{\gamma}{2}} \int_{-\infty+i\epsilon}^{\infty+i\epsilon} dx e^{-iz'x} \frac{\Gamma(-ix)}{\Gamma(ix)} \\ &= \Theta(z') \frac{\mathcal{I}_0(z')}{\sin^2 \frac{\gamma}{2}} \end{aligned} \quad (\text{A.13})$$

where

$$z' = \frac{u - v'}{2M} - 2 \ln \left| \sin \frac{\gamma}{2} \right|. \quad (\text{A.14})$$

---

<sup>14</sup>Please find the associated glory effects in [108, 109].

The critical equation in this case is

$$z' = \frac{u - v'}{2M} - 2 \ln \left| \sin \frac{\gamma}{2} \right| = 0 \quad (\text{A.15})$$

which is approximately the same as (2.79) up to an IR regulator.

## B The equation from $\mathcal{I}^-$ to $\mathcal{I}^+$

In this appendix, we will investigate the properties of the function  $h(\gamma)$  in (3.16). When the impact parameter is large, we can prove that  $r_0$  is large via (3.11). As a matter of fact,

$$b = \frac{r_0}{\sqrt{A(r_0)}} = r_0(1 + \mathcal{R}^{-1} + \mathcal{O}(\mathcal{R}^{-2})), \quad r_0 \rightarrow \infty. \quad (\text{B.1})$$

We have defined dimensionless parameter

$$\mathcal{R} = \frac{r_0}{M}. \quad (\text{B.2})$$

The equation (3.14) can be expanded in large  $r_0$  limit

$$u - v' = -4M \ln \mathcal{R} + 2M(1 + 2\zeta + 2 \ln 4 + 2 \ln(\zeta - 1)) + \mathcal{O}(\mathcal{R}^{-1}), \quad (\text{B.3a})$$

$$\gamma = \frac{4}{\mathcal{R}} + \mathcal{O}(\mathcal{R}^{-2}). \quad (\text{B.3b})$$

As a consequence, we find

$$\frac{u - v'}{M} = 4 \ln \gamma + 2 + 4\zeta + 4 \ln(\zeta - 1) + \mathcal{O}(\gamma). \quad (\text{B.4})$$

The result can be extended to a general spherically symmetric in an asymptotically flat space-time. The general line element is described by

$$ds^2 = -A(r)dt^2 + B(r)dr^2 + C(r)(d\theta^2 + \sin^2 \theta d\phi^2) \quad (\text{B.5})$$

in which  $A(r)$ ,  $B(r)$  and  $C(r)$  satisfy an asymptotically flat condition

$$\lim_{r \rightarrow \infty} A(r) = 1, \quad \lim_{r \rightarrow \infty} B(r) = 1, \quad \lim_{r \rightarrow \infty} C(r) = r^2. \quad (\text{B.6})$$

Note that one can always redefine the radius  $r$  to set  $C = r^2$ . The tortoise coordinate is

$$r_*(r) = \int_o^r dr' \sqrt{\frac{B(r')}{A(r')}}. \quad (\text{B.7})$$

However, we will keep this function in this work. A straightforward derivation leads to

$$u - v' = 2 \int_{r_0}^{\infty} dr \sqrt{\frac{B}{A}} \left( \frac{1}{\sqrt{1 - \frac{Ab^2}{C}}} - 1 \right) - 2r_*(r_0), \quad (\text{B.8a})$$

$$\phi - \phi' = 2 \int_{r_0}^{\infty} dr \sqrt{\frac{B}{C}} \frac{1}{\sqrt{\frac{C}{Ab^2} - 1}}. \quad (\text{B.8b})$$

The turning point  $r_0$  is related to  $b$  via

$$b^2 = \frac{C(r_0)}{A(r_0)}. \quad (\text{B.9})$$

When  $r_0 \rightarrow \infty$ , the functions  $A, B, C$  are expanded as

$$A(r) = 1 + \frac{a_{-1}}{r} + \dots, \quad B(r) = 1 + \frac{b_{-1}}{r} + \dots, \quad C(r) = r^2 + c_1 r + \dots. \quad (\text{B.10})$$

Then we find

$$u - v' = -(b_{-1} - a_{-1}) \ln r_0 + c_1 - a_{-1} + (b_{-1} - a_{-1}) \ln 2o + 2o + \dots, \quad (\text{B.11a})$$

$$\phi - \phi' = \pi + \frac{b_{-1} - a_{-1}}{r_0} + \dots. \quad (\text{B.11b})$$

The turning point is approximately equal to the impact parameter

$$b = r_0 + \frac{c_1 - a_{-1}}{2} + \mathcal{O}(r_0^{-1}). \quad (\text{B.12})$$

Therefore, the relation between the time delay and the deflection angle is

$$u - v' = (b_{-1} - a_{-1}) \ln \gamma + (b_{-1} - a_{-1}) \ln \frac{2o}{b_{-1} - a_{-1}} + c_1 - a_{-1} + 2o + \mathcal{O}(\gamma). \quad (\text{B.13})$$

The logarithmic behavior only depends on the coefficient  $b_{-1} - a_{-1}$  which is the same for both Schwarzschild and RN black holes.

In the opposite limit,  $\gamma \rightarrow \infty$ , we should deal with the strong field region. The light deflection in the strong field region has been discussed in [73] and we will adopt a similar method as in [111] in this appendix. We still use the metric (B.5). We assume the photon sphere is located at  $r_{ps}$  and thus obeys the equation

$$D(r) \equiv \frac{C'(r)}{C(r)} - \frac{A'(r)}{A(r)} \Big|_{r=r_{ps}} = 0. \quad (\text{B.14})$$

We define a function

$$K(r) = \frac{C}{Ab^2} - 1 = \frac{C(r)A(r_0)}{A(r)C(r_0)} - 1 \quad (\text{B.15})$$

that satisfies the condition

$$K(r_0) = 0. \quad (\text{B.16})$$

The equation (B.8) can be written as

$$u - v' = 2 \int_{r_0}^{\infty} dr \sqrt{\frac{B}{A}} \frac{1}{\sqrt{K} (\sqrt{K+1} + \sqrt{K})} - 2r_*(r_0), \quad (\text{B.17a})$$

$$\phi - \phi' = 2 \int_{r_0}^{\infty} dr \sqrt{\frac{B}{CK}}. \quad (\text{B.17b})$$

When  $r_0 \rightarrow r_{ps}$ , the integral may be divergent. Therefore, we change the variable  $r = \frac{r_0}{1-x}$  with  $0 < x < 1$ . Then

$$K(r) = K\left(\frac{r_0}{1-x}\right) = K_1(r_0)x + K_2(r_0)x^2 + \dots \quad (\text{B.18})$$

where

$$K_1(r_0) = r_0 D_0, \quad (\text{B.19a})$$

$$K_2(r_0) = \frac{1}{2} r_0 (D_0^2 r_0 + 2D_0 + r_0 D_0') \quad (\text{B.19b})$$

where  $D_0 = D(r_0)$ ,  $D_0' = \frac{d}{dr_0} D(r_0)$ . When  $r_0 \rightarrow r_{ps}$ , we have

$$D_0 = D(r_{ps}) + D'(r_{ps})(r_0 - r_{ps}) + \dots = D'_{ps}(r_0 - r_{ps}) + \dots \quad (\text{B.20})$$

with

$$D'_{ps} = \left. \frac{dD(r_0)}{dr_0} \right|_{r_0=r_{ps}}. \quad (\text{B.21})$$

Expanding  $K_1(r_0)$  and  $K_2(r_0)$  around  $r_{ps}$ , we find

$$K_1(r_0) = r_{ps} D'_{ps} (r_0 - r_{ps}) + \dots, \quad K_2(r_0) = \frac{1}{2} r_{ps}^2 D'_{ps} + \dots \quad (\text{B.22})$$

The integrals (B.17) are improper integrals and they diverge logarithmically

$$u - v' \sim \ln(r_0 - r_{ps}), \quad (\text{B.23a})$$

$$\phi - \phi' \sim \ln(r_0 - r_{ps}). \quad (\text{B.23b})$$

We use the limit comparison test (LCT) for improper integrals to find the ratio

$$\lim_{r \rightarrow r_{ps}} \frac{\sqrt{\frac{B}{A}} \frac{1}{\sqrt{K}(\sqrt{K+1}+\sqrt{K})}}{\sqrt{\frac{B}{CK}}} = \sqrt{\frac{C(r_{ps})}{A(r_{ps})}} = b_c \quad (\text{B.24})$$

where  $b_c$  is the critical impact parameter. Thus, we prove the linear relation

$$u - v' = b_c \gamma + \dots \quad (\text{B.25})$$

To determine the constant, we should compute (B.23) more precisely

$$u - v' = 2r_0 \int_0^1 \frac{dx}{\sqrt{G(r_0, x)}} - 2r_*(r_0), \quad (\text{B.26a})$$

$$\phi - \phi' = 2r_0 \int_0^1 \frac{dx}{\sqrt{F(r_0, x)}} \quad (\text{B.26b})$$

where

$$G(r_0, x) = (1-x)^4 \frac{A}{B} K \left( \sqrt{K} + \sqrt{K+1} \right)^2, \quad (\text{B.27a})$$

$$F(r_0, x) = (1-x)^4 \frac{CK}{B}. \quad (\text{B.27b})$$

Note that the functions are evaluated at  $r = \frac{r_0}{1-x}$ . Now it is straightforward to find the asymptotic expansion

$$G(r_0, x) = g_1 x + g_{\frac{3}{2}} x^{\frac{3}{2}} + g_2 x^2 + \dots, \quad (\text{B.28a})$$

$$F(r_0, x) = f_1 x + f_2 x^2 + \dots \quad (\text{B.28b})$$

where

$$f_1 = \frac{K_1(r_0)C(r_0)}{B(r_0)} = \frac{r_{ps} D'_{ps} C_{ps}}{B_{ps}} (r_0 - r_{ps}) + \dots, \quad (\text{B.29a})$$

$$f_2 = \frac{K_2(r_0)C(r_0)}{B(r_0)} + K_1(r_0) \times (\dots) = \frac{r_{ps}^2 D'_{ps} C_{ps}}{2B_{ps}} + \dots, \quad (\text{B.29b})$$

$$g_1 = \frac{K_1(r_0)A(r_0)}{B(r_0)} = \frac{r_{ps} D'_{ps} A_{ps}}{B_{ps}} (r_0 - r_{ps}) + \dots, \quad (\text{B.29c})$$

$$g_{\frac{3}{2}} = \frac{2K_1^{\frac{3}{2}}(r_0)A(r_0)}{B(r_0)} = \dots, \quad (\text{B.29d})$$

$$g_2 = \frac{K_2(r_0)A(r_0)}{B(r_0)} + K_1(r_0) \times (\dots) = \frac{r_{ps}^2 D'_{ps} A_{ps}}{2B_{ps}} + \dots. \quad (\text{B.29e})$$

The terms denoted by  $\dots$  are not important for extracting the logarithmic behavior, so we do not write them out explicitly. The subscript “ps” denotes the value of the corresponding function at the photon sphere.

We define the divergent part as

$$\mathcal{I}_D = 2r_0 \int_0^1 \frac{dx}{\sqrt{g_1 x + g_{\frac{3}{2}} x^{\frac{3}{2}} + g_2 x^2}} = \frac{4r_0}{\sqrt{g_2}} \ln \left( \frac{2\sqrt{g_1 g_2} - g_{\frac{3}{2}}}{2\sqrt{g_2}(g_1 + g_2 + g_{\frac{3}{2}}) - 2g_2 - g_{\frac{3}{2}}} \right), \quad (\text{B.30a})$$

$$\mathcal{J}_D = 2r_0 \int_0^1 \frac{dx}{\sqrt{f_1 x + f_2 x^2}} = \frac{4r_0}{\sqrt{f_2}} \ln \left( \frac{\sqrt{f_1}}{\sqrt{f_1 + f_2} - \sqrt{f_2}} \right) \quad (\text{B.30b})$$

and separate the integrals (B.26) into divergent and convergent part

$$u - v' = \mathcal{I}_D + \mathcal{I}_C, \quad (\text{B.31a})$$

$$\gamma = \mathcal{J}_D + \mathcal{J}_C \quad (\text{B.31b})$$

where

$$\mathcal{I}_C = 2r_0 \int_0^1 dx \left( \frac{1}{\sqrt{G(r_0, x)}} - \frac{1}{\sqrt{g_1 x + g_{\frac{3}{2}} x^{\frac{3}{2}} + g_2 x^2}} \right) - 2r_*(r_0), \quad (\text{B.32a})$$

$$\mathcal{J}_C = 2r_0 \int_0^1 dx \left( \frac{1}{\sqrt{F(r_0, x)}} - \frac{1}{\sqrt{f_1 x + f_2 x^2}} \right) - \pi. \quad (\text{B.32b})$$

Utilizing (B.29), we find

$$\mathcal{I}_D = \frac{2r_{ps}}{\sqrt{g_2(r_{ps})}} \ln \frac{2r_{ps}}{(r_0 - r_{ps})} + \dots, \quad (\text{B.33a})$$

$$\mathcal{J}_D = \frac{2r_{ps}}{\sqrt{f_2(r_{ps})}} \ln \frac{2r_{ps}}{(r_0 - r_{ps})} + \dots. \quad (\text{B.33b})$$

The ratio of the coefficients is

$$\lim_{r_0 \rightarrow r_{ps}} \frac{u - v'}{\gamma} = \lim_{r_0 \rightarrow r_{ps}} \frac{\mathcal{I}_D}{\mathcal{J}_D} = \sqrt{\frac{f_2(r_{ps})}{g_2(r_{ps})}} = \sqrt{\frac{C_{ps}}{A_{ps}}} = b_c \quad (\text{B.34})$$

which is consistent with (B.25). Thus, the time delay and the deflection angle in the strong field limit is

$$u - v' = -\frac{2r_{ps}}{\sqrt{g_2(r_{ps})}} \ln \frac{r_0 - r_{ps}}{2r_{ps}} + \mathcal{I}_C + \mathcal{O}(r_0 - r_{ps}), \quad (\text{B.35a})$$

$$\gamma = -\frac{2r_{ps}}{\sqrt{f_2(r_{ps})}} \ln \frac{r_0 - r_{ps}}{2r_{ps}} + \mathcal{J}_C + \mathcal{O}(r_0 - r_{ps}). \quad (\text{B.35b})$$

As a consequence,

$$u - v' = b_c \gamma + \mathcal{I}_C - b_c \mathcal{J}_C + \mathcal{O}(r_0 - r_{ps}). \quad (\text{B.36})$$

This is a linear function and we can find the constant

$$c_0 = \frac{\mathcal{I}_C - b_c \mathcal{J}_C}{M} \Big|_{r_0=r_{ps}}. \quad (\text{B.37})$$

Note that the logarithmic divergence can be written as

$$\mathcal{I}_D = -\sqrt{\frac{2B_{ps}}{A_{ps}D'_{ps}}} \ln \left( \frac{b_0}{b_c} - 1 \right) + \sqrt{\frac{2B_{ps}}{A_{ps}D'_{ps}}} \ln (D'_{ps} r_{ps}^2) + \dots, \quad (\text{B.38a})$$

$$\mathcal{J}_D = -\sqrt{\frac{2B_{ps}}{C_{ps}D'_{ps}}} \ln \left( \frac{b_0}{b_c} - 1 \right) + \sqrt{\frac{2B_{ps}}{C_{ps}D'_{ps}}} \ln (D'_{ps} r_{ps}^2) + \dots. \quad (\text{B.38b})$$

alternatively using the identity

$$\frac{b_0 - b_c}{b_c} = \frac{\sqrt{\frac{C(r_0)}{A(r_0)}} - \sqrt{\frac{C_{ps}}{A_{ps}}}}{\sqrt{\frac{C_{ps}}{A_{ps}}}} = \frac{1}{4} D'_{ps} (r_0 - r_{ps})^2. \quad (\text{B.39})$$

For the Schwarzschild black hole, we find

$$\mathcal{I}_D = -3\sqrt{3}M \ln \left( \frac{b_0}{b_c} - 1 \right) + 3\sqrt{3}M \ln 6, \quad (\text{B.40a})$$

$$\mathcal{J}_D = -\ln \left( \frac{b_0}{b_c} - 1 \right) + \ln 6. \quad (\text{B.40b})$$

Furthermore,

$$G(r_{ps}, x) = \frac{1}{9} x^2 (3 - 2x) \left( \sqrt{(3 - 2x)x^2 + 1} \right)^2, \quad (\text{B.41a})$$

$$F(r_{ps}, x) = 3M^2 (3 - 2x)x^2, \quad (\text{B.41b})$$

$$f_2(r_{ps}) = 9M^2, \quad g_2(r_{ps}) = \frac{1}{3}. \quad (\text{B.41c})$$

We find

$$\mathcal{J}_C \Big|_{r_0=r_{ps}} = 2 \ln (12 - 6\sqrt{3}) - \pi. \quad (\text{B.42})$$

Similarly,

$$\mathcal{I}_C \Big|_{r_0=r_{ps}} = 2M \left( -3\sqrt{3} + 3 + \ln (5404 - 3120\sqrt{3}) - 6\sqrt{3} \ln (\sqrt{3} + 1) + 3\sqrt{3} \ln(12) + 2 \ln 2 \right)$$

$$+ 4M (\zeta + \ln(\zeta - 1)). \quad (\text{B.43})$$

With the standard choice of the reference point, we find

$$c_0 \approx 1.674. \quad (\text{B.44})$$

We checked this result numerically.

## C The equation from $\mathcal{I}^-$ to $\mathcal{H}^+$

To prove the hyperbola behaviour in the small  $b$  limit, we expand the integrals directly

$$\frac{v - v'}{M} = \frac{b^2}{4} + \mathcal{O}(b^4), \quad (\text{C.1a})$$

$$\phi - \phi' = \frac{b}{2} + \mathcal{O}(b^3). \quad (\text{C.1b})$$

Thus they obey the law

$$\frac{v - v'}{M} = \gamma^2 + \mathcal{O}(\gamma^4). \quad (\text{C.2})$$

Now in the limit  $b \rightarrow b_c^-$ , both of the integrals (3.32) diverge logarithmically

$$v - v' \sim \ln \left( 1 - \frac{b}{b_c} \right), \quad \phi - \phi' \sim \ln \left( 1 - \frac{b}{b_c} \right). \quad (\text{C.3})$$

We can still use the limit comparison test for improper integrals to find the ratio

$$\lim_{r \rightarrow r_{ps}} \frac{\frac{1 - \sqrt{1 - \frac{A(r)b^2}{r^2}}}{A(r)\sqrt{1 - \frac{A(r)b^2}{r^2}}}}{\frac{1}{r\sqrt{\frac{r^2}{b^2} - A(r)}}} = 3\sqrt{3}M. \quad (\text{C.4})$$

This fixes the coefficient  $3\sqrt{3}$  in (3.37). The constant  $\tilde{c}_0$  can be found by taking the limit

$$\tilde{c}_0 = \lim_{b \rightarrow b_c^-} \left( \frac{v - v'}{M} - 3\sqrt{3}(\phi - \phi') \right) \approx -8.878. \quad (\text{C.5})$$

## References

- [1] **LIGO Scientific, Virgo** Collaboration, B. P. Abbott *et al.*, “Observation of Gravitational Waves from a Binary Black Hole Merger,” *Phys. Rev. Lett.* **116** (2016), no. 6, 061102, [1602.03837](https://arxiv.org/abs/1602.03837).

- [2] L. Blanchet, “Post-Newtonian Theory for Gravitational Waves,” *Living Rev. Rel.* **17** (2014) 2, [1310.1528](#).
- [3] T. Damour, “Coalescence of two spinning black holes: an effective one-body approach,” *Phys. Rev. D* **64** (2001) 124013, [gr-qc/0103018](#).
- [4] W. D. Goldberger and I. Z. Rothstein, “An Effective field theory of gravity for extended objects,” *Phys. Rev. D* **73** (2006) 104029, [hep-th/0409156](#).
- [5] Z. Bern, C. Cheung, R. Roiban, C.-H. Shen, M. P. Solon, and M. Zeng, “Scattering Amplitudes and the Conservative Hamiltonian for Binary Systems at Third Post-Minkowskian Order,” *Phys. Rev. Lett.* **122** (2019), no. 20, 201603, [1901.04424](#).
- [6] H. Bondi, M. G. J. van der Burg, and A. W. K. Metzner, “Gravitational waves in general relativity. 7. Waves from axisymmetric isolated systems,” *Proc. Roy. Soc. Lond. A* **269** (1962) 21–52.
- [7] R. K. Sachs, “Gravitational waves in general relativity. 8. Waves in asymptotically flat space-times,” *Proc. Roy. Soc. Lond. A* **270** (1962) 103–126.
- [8] G. Barnich and C. Troessaert, “Aspects of the BMS/CFT correspondence,” *JHEP* **05** (2010) 062, [1001.1541](#).
- [9] A. Bagchi, A. Banerjee, P. Dhivakar, S. Mondal, and A. Shukla, “The Carrollian Kaleidoscope,” [2506.16164](#).
- [10] L. Donnay, A. Fiorucci, Y. Herfray, and R. Ruzziconi, “Carrollian Perspective on Celestial Holography,” *Phys. Rev. Lett.* **129** (2022), no. 7, 071602, [2202.04702](#).
- [11] L. Donnay, A. Fiorucci, Y. Herfray, and R. Ruzziconi, “Bridging Carrollian and celestial holography,” *Phys. Rev. D* **107** (2023), no. 12, 126027, [2212.12553](#).
- [12] A. Bagchi, S. Banerjee, R. Basu, and S. Dutta, “Scattering Amplitudes: Celestial and Carrollian,” *Phys. Rev. Lett.* **128** (2022), no. 24, 241601, [2202.08438](#).
- [13] L. Mason, R. Ruzziconi, and A. Yellespur Srikant, “Carrollian Amplitudes and Celestial Symmetries,” [2312.10138](#).
- [14] W.-B. Liu, J. Long, and X.-Q. Ye, “Feynman rules and loop structure of Carrollian amplitudes,” *JHEP* **05** (2024) 213, [2402.04120](#).
- [15] A. Li, J. Long, and J.-L. Yang, “Carrollian propagator and amplitude in Rindler spacetime,” *JHEP* **03** (2025) 186, [2410.20372](#).
- [16] W.-B. Liu, J. Long, H.-Y. Xiao, and J.-L. Yang, “On the definition of Carrollian amplitudes in general dimensions,” *JHEP* **11** (2024) 027, [2407.20816](#).

- [17] K. Nguyen, “Carrollian conformal correlators and massless scattering amplitudes,” *Journal of High Energy Physics* **2024** (2024), no. 1, 76.
- [18] H. Kulkarni, R. Ruzziconi, and A. Y. Srikant, “On carrollian and celestial correlators in general dimensions,” *Journal of High Energy Physics* **2025** (2025), no. 10, 1–36.
- [19] J. Long and J.-L. Yang, “Constraining bulk-to-boundary correlators in the theories with Poincaré symmetry,” [2601.18461](#).
- [20] R. F. Penna, “BMS invariance and the membrane paradigm,” *JHEP* **03** (2016) 023, [1508.06577](#).
- [21] L. Ciambelli, C. Marateau, A. C. Petkou, P. M. Petropoulos, and K. Siampos, “Flat holography and Carrollian fluids,” *JHEP* **07** (2018) 165, [1802.06809](#).
- [22] L. Ciambelli, C. Marateau, A. C. Petkou, P. M. Petropoulos, and K. Siampos, “Covariant Galilean versus Carrollian hydrodynamics from relativistic fluids,” *Class. Quant. Grav.* **35** (2018), no. 16, 165001, [1802.05286](#).
- [23] L. Donnay and C. Marateau, “Carrollian Physics at the Black Hole Horizon,” *Class. Quant. Grav.* **36** (2019), no. 16, 165002, [1903.09654](#).
- [24] A. C. Petkou, P. M. Petropoulos, D. Rivera-Betancour, and K. Siampos, “Relativistic fluids, hydrodynamic frames and their galilean versus carrollian avatars,” *Journal of High Energy Physics* **2022** (2022), no. 9, 162.
- [25] L. Freidel and P. Jai-akson, “Carrollian hydrodynamics from symmetries,” *Classical and Quantum Gravity* **40** (2023), no. 5, 055009.
- [26] J. Armas and E. Have, “Carrollian fluids and spontaneous breaking of boost symmetry,” *Physical Review Letters* **132** (2024), no. 16, 161606.
- [27] J. Long and X.-H. Zhou, “Reduction of topological invariants on null hypersurfaces,” *JHEP* **01** (2026) 116, [2509.06073](#).
- [28] W.-B. Liu, J. Long, and X.-H. Zhou, “Electromagnetic helicity flux operators in higher dimensions,” *JHEP* **04** (2025) 026, [2407.20077](#).
- [29] J. Long and R.-Z. Yu, “Gravitational helicity flux density from two-body systems,” *Class. Quant. Grav.* **42** (2025), no. 4, 045005, [2403.18627](#).
- [30] Z.-Y. Heng, J. Long, R.-Z. Yu, and X.-H. Zhou, “Electromagnetic helicity flux density for radiative systems,” *Class. Quant. Grav.* **43** (2026), no. 1, 015016, [2507.14966](#).
- [31] J. Long and H.-Y. Xiao, “Thermal correlator at null infinity,” *JHEP* **10** (2025) 127, [2501.15714](#).

- [32] T. Regge and J. A. Wheeler, “Stability of a Schwarzschild singularity,” *Phys. Rev.* **108** (1957) 1063–1069.
- [33] F. J. Zerilli, “Effective potential for even parity Regge-Wheeler gravitational perturbation equations,” *Phys. Rev. Lett.* **24** (1970) 737–738.
- [34] E. Newman and R. Penrose, “An Approach to gravitational radiation by a method of spin coefficients,” *J. Math. Phys.* **3** (1962) 566–578.
- [35] S. A. Teukolsky, “Perturbations of a Rotating Black Hole. I. Fundamental Equations for Gravitational, Electromagnetic, and Neutrino-Field Perturbations,” *Astrophysics Journal* **185** (Oct., 1973) 635–648.
- [36] A. Pound and B. Wardell, “Black hole perturbation theory and gravitational self-force,” [2101.04592](#).
- [37] C. V. Vishveshwara, “Scattering of Gravitational Radiation by a Schwarzschild Black-hole,” *Nature* **227** (1970) 936–938.
- [38] R. H. Price, “Nonspherical Perturbations of Relativistic Gravitational Collapse. II. Integer-Spin, Zero-Rest-Mass Fields,” *Phys. Rev. D* **5** (1972) 2439–2454.
- [39] E. S. C. Ching, P. T. Leung, W. M. Suen, and K. Young, “Wave propagation in gravitational systems: Late time behavior,” *Phys. Rev. D* **52** (1995) 2118–2132, [gr-qc/9507035](#).
- [40] A. A. Starobinskii and S. M. Churilov, “Amplification of electromagnetic and gravitational waves scattered by a rotating “black hole”,” *Soviet Journal of Experimental and Theoretical Physics* **38** (Jan., 1974) 1.
- [41] G. W. Gibbons, “Vacuum polarization and the spontaneous loss of charge by black holes,” *Communications in Mathematical Physics* **44** (Oct., 1975) 245–264.
- [42] D. N. Page, “Particle Emission Rates from a Black Hole: Massless Particles from an Uncharged, Nonrotating Hole,” *Phys. Rev. D* **13** (1976) 198–206.
- [43] W. G. Unruh, “Absorption Cross-Section of Small Black Holes,” *Phys. Rev. D* **14** (1976) 3251–3259.
- [44] N. G. Sanchez, “Absorption and Emission Spectra of a Schwarzschild Black Hole,” *Phys. Rev. D* **18** (1978) 1030.
- [45] S. R. Das, G. W. Gibbons, and S. D. Mathur, “Universality of low-energy absorption cross-sections for black holes,” *Phys. Rev. Lett.* **78** (1997) 417–419, [hep-th/9609052](#).

- [46] N. Andersson, “Evolving test fields in a black hole geometry,” *Phys. Rev. D* **55** (1997) 468–479, [gr-qc/9607064](#).
- [47] P. Arnaudo, J. Carballo, and B. Withers, “Beyond quasinormal modes: a complete mode decomposition of black hole perturbations,” [2510.18956](#).
- [48] D. T. Son and A. O. Starinets, “Minkowski space correlators in AdS / CFT correspondence: Recipe and applications,” *JHEP* **09** (2002) 042, [hep-th/0205051](#).
- [49] L. F. Alday, M. Nocchi, R. Ruzziconi, and A. Yellespur Srikant, “Carrollian Amplitudes from Holographic Correlators,” [2406.19343](#).
- [50] G. Aminov, A. Grassi, and Y. Hatsuda, “Black Hole Quasinormal Modes and Seiberg–Witten Theory,” *Annales Henri Poincaré* **23** (2022), no. 6, 1951–1977, [2006.06111](#).
- [51] G. Bonelli, C. Iossa, D. P. Lichtig, and A. Tanzini, “Exact solution of Kerr black hole perturbations via CFT2 and instanton counting: Greybody factor, quasinormal modes, and Love numbers,” *Phys. Rev. D* **105** (2022), no. 4, 044047, [2105.04483](#).
- [52] G. Bonelli, C. Iossa, D. Panea Lichtig, and A. Tanzini, “Irregular Liouville Correlators and Connection Formulae for Heun Functions,” *Commun. Math. Phys.* **397** (2023), no. 2, 635–727, [2201.04491](#).
- [53] V. Frolov and I. Novikov, *Black hole physics: Basic concepts and new developments*, vol. 96. Springer Science & Business Media, 2012.
- [54] C. Gundlach, R. H. Price, and J. Pullin, “Late time behavior of stellar collapse and explosions: 1. Linearized perturbations,” *Phys. Rev. D* **49** (1994) 883–889, [gr-qc/9307009](#).
- [55] R. H. Price, “Nonspherical perturbations of relativistic gravitational collapse. 1. Scalar and gravitational perturbations,” *Phys. Rev. D* **5** (1972) 2419–2438.
- [56] H. D. I. Abarbanel and C. Itzykson, “Relativistic eikonal expansion,” *Phys. Rev. Lett.* **23** (1969) 53.
- [57] M. Levy and J. Sucher, “Eikonal approximation in quantum field theory,” *Phys. Rev.* **186** (1969) 1656–1670.
- [58] H. Cheng and T. T. Wu, “High-energy elastic scattering in quantum electrodynamics,” *Phys. Rev. Lett.* **22** (1969) 666.
- [59] S. J. Wallace, “Eikonal expansion,” *Annals Phys.* **78** (1973) 190–257.

- [60] P. C. Aichelburg and R. U. Sexl, “On the Gravitational field of a massless particle,” *Gen. Rel. Grav.* **2** (1971) 303–312.
- [61] T. Dray and G. ’t Hooft, “The Gravitational Shock Wave of a Massless Particle,” *Nucl. Phys. B* **253** (1985) 173–188.
- [62] G. ’t Hooft, “Graviton Dominance in Ultrahigh-Energy Scattering,” *Phys. Lett. B* **198** (1987) 61–63.
- [63] D. Amati, M. Ciafaloni, and G. Veneziano, “Superstring Collisions at Planckian Energies,” *Phys. Lett. B* **197** (1987) 81.
- [64] T. Adamo, A. Cristofoli, and P. Tourkine, “Eikonal amplitudes from curved backgrounds,” *SciPost Phys.* **13** (2022), no. 2, 032, [2112.09113](#).
- [65] W.-B. Liu and J. Long, “Extrapolating the massive fields to future timelike infinity,” *JHEP* **12** (2025) 042, [2508.15619](#).
- [66] T. Adamo, W. Bu, P. Tourkine, and B. Zhu, “Eikonal amplitudes on the celestial sphere,” *Journal of High Energy Physics* **2024** (Oct., 2024) 192, [2405.15594](#).
- [67] S. Weinberg, *Gravitation and Cosmology: Principles and Applications of the General Theory of Relativity*. 1972.
- [68] J. J. Duistermaat and L. Hörmander, “Fourier integral operators. ii,” in *Mathematics Past and Present Fourier Integral Operators*, pp. 129–215. Springer, 1994.
- [69] L. Hörmander, *The analysis of linear partial differential operators IV: Fourier integral operators*. Springer, 2009.
- [70] E. Poisson, A. Pound, and I. Vega, “The Motion of point particles in curved spacetime,” *Living Rev. Rel.* **14** (2011) 7, [1102.0529](#).
- [71] A. I. Harte and T. D. Drivas, “Caustics and wave propagation in curved spacetimes,” *Phys. Rev. D* **85** (2012) 124039, [1202.0540](#).
- [72] A. Zenginoglu and C. R. Galley, “Caustic echoes from a Schwarzschild black hole,” *Phys. Rev. D* **86** (2012) 064030, [1206.1109](#).
- [73] V. Bozza, “Gravitational lensing in the strong field limit,” *Physical Review D* **66** (2002), no. 10, 103001.
- [74] V. Bozza and L. Mancini, “Time delay in black hole gravitational lensing as a distance estimator,” *General Relativity and Gravitation* **36** (2004), no. 2, 435–450.

- [75] G. Muñoz, “Orbits of massless particles in the Schwarzschild metric: Exact solutions,” *American Journal of Physics* **82** (June, 2014) 564–573.
- [76] S. E. Gralla and A. Lupsasca, “Null geodesics of the Kerr exterior,” *Phys. Rev. D* **101** (2020), no. 4, 044032, [1910.12881](#).
- [77] G. W. Gibbons and M. Vyska, “The Application of Weierstrass elliptic functions to Schwarzschild Null Geodesics,” *Class. Quant. Grav.* **29** (2012) 065016, [1110.6508](#).
- [78] V. Ferrari and B. Mashhoon, “New approach to the quasinormal modes of a black hole,” *Phys. Review D* **30** (July, 1984) 295–304.
- [79] C. J. Goebel, “Comments on the “vibrations” of a Black Hole.,” *Astrophysics Journal* **172** (Mar., 1972) L95.
- [80] H.-J. Blome and B. Mashhoon, “Quasi-normal oscillations of a schwarzschild black hole,” *Phys. Lett. A* **100** (1981), no. 5, 231–234.
- [81] B. F. Schutz and C. M. Will, “BLACK HOLE NORMAL MODES: A SEMIANALYTIC APPROACH,” *Astrophys. J. Lett.* **291** (1985) L33–L36.
- [82] E. W. Leaver, “An Analytic representation for the quasi normal modes of Kerr black holes,” *Proc. Roy. Soc. Lond. A* **402** (1985) 285–298.
- [83] E. W. Leaver, “Spectral decomposition of the perturbation response of the Schwarzschild geometry,” *Phys. Rev. D* **34** (1986) 384–408.
- [84] S. Mano, H. Suzuki, and E. Takasugi, “Analytic solutions of the Teukolsky equation and their low frequency expansions,” *Prog. Theor. Phys.* **95** (1996) 1079–1096, [gr-qc/9603020](#).
- [85] M. Sasaki and H. Tagoshi, “Analytic black hole perturbation approach to gravitational radiation,” *Living Rev. Rel.* **6** (2003) 6, [gr-qc/0306120](#).
- [86] J. Abedi *et al.*, “Black hole spectroscopy: from theory to experiment,” [2505.23895](#).
- [87] S. R. Dolan and A. C. Ottewill, “Wave Propagation and Quasinormal Mode Excitation on Schwarzschild Spacetime,” *Phys. Rev. D* **84** (2011) 104002, [1106.4318](#).
- [88] H. Yang, D. A. Nichols, F. Zhang, A. Zimmerman, Z. Zhang, and Y. Chen, “Quasinormal-mode spectrum of kerr black holes and its geometric interpretation,” *Phys. Rev. D* **86** (Nov, 2012) 104006.
- [89] E. Berti, V. Cardoso, and A. O. Starinets, “Quasinormal modes of black holes and black branes,” *Class. Quant. Grav.* **26** (2009) 163001, [0905.2975](#).

- [90] S. W. Hawking, M. J. Perry, and A. Strominger, “Soft Hair on Black Holes,” *Phys. Rev. Lett.* **116** (2016), no. 23, 231301, [1601.00921](#).
- [91] G. Compère and J. Long, “Vacua of the gravitational field,” *JHEP* **07** (2016) 137, [1601.04958](#).
- [92] G. Compère and J. Long, “Classical static final state of collapse with supertranslation memory,” *Class. Quant. Grav.* **33** (2016), no. 19, 195001, [1602.05197](#).
- [93] K. Mitman *et al.*, “A review of gravitational memory and BMS frame fixing in numerical relativity,” *Class. Quant. Grav.* **41** (2024), no. 22, 223001, [2405.08868](#).
- [94] K. Mitman *et al.*, “Fixing the BMS frame of numerical relativity waveforms,” *Phys. Rev. D* **104** (2021), no. 2, 024051, [2105.02300](#).
- [95] L. Magaña Zertuche *et al.*, “High precision ringdown modeling: Multimode fits and BMS frames,” *Phys. Rev. D* **105** (2022), no. 10, 104015, [2110.15922](#).
- [96] A. Strominger, “On BMS Invariance of Gravitational Scattering,” *JHEP* **07** (2014) 152, [1312.2229](#).
- [97] S. Chandrasekhar, *The mathematical theory of black holes*. 1985.
- [98] G. Compère, Y. Liu, and J. Long, “Classification of radial Kerr geodesic motion,” *Phys. Rev. D* **105** (2022), no. 2, 024075, [2106.03141](#).
- [99] Y. B. Zel’Dovich, “Generation of Waves by a Rotating Body,” *Soviet Journal of Experimental and Theoretical Physics Letters* **14** (Aug., 1971) 180.
- [100] J. D. Bekenstein and M. Schiffer, “The Many faces of superradiance,” *Phys. Rev. D* **58** (1998) 064014, [gr-qc/9803033](#).
- [101] R. Brito, V. Cardoso, and P. Pani, “Superradiance: New Frontiers in Black Hole Physics,” *Lect. Notes Phys.* **906** (2015) pp.1–237, [1501.06570](#).
- [102] R. J. Gleiser, C. O. Nicasio, R. H. Price, and J. Pullin, “Second order perturbations of a Schwarzschild black hole,” *Class. Quant. Grav.* **13** (1996) L117–L124, [gr-qc/9510049](#).
- [103] M. Campanelli and C. O. Lousto, “Second order gauge invariant gravitational perturbations of a Kerr black hole,” *Phys. Rev. D* **59** (1999) 124022, [gr-qc/9811019](#).
- [104] B. S. DeWitt and R. W. Brehme, “Radiation damping in a gravitational field,” *Annals Phys.* **9** (1960) 220–259.
- [105] N. Andersson and B. P. Jensen, “Scattering by black holes. Chapter 0.1,” [gr-qc/0011025](#).

- [106] Y. Decanini, G. Esposito-Farese, and A. Folacci, “Universality of high-energy absorption cross sections for black holes,” *Phys. Rev. D* **83** (2011) 044032, [1101.0781](#).
- [107] K. Glampedakis and N. Andersson, “Scattering of scalar waves by rotating black holes,” *Class. Quant. Grav.* **18** (2001) 1939–1966, [gr-qc/0102100](#).
- [108] P. Anninos, C. DeWitt-Morette, R. A. Matzner, P. Yioutas, and T. R. Zhang, “Orbiting cross-sections: Application to black hole scattering,” *Phys. Rev. D* **46** (1992) 4477–4494.
- [109] Y. Nambu and S. Noda, “Wave Optics in Black Hole Spacetimes: Schwarzschild Case,” *Class. Quant. Grav.* **33** (2016) 075011, [1502.05468](#).
- [110] J. A. H. Futterman, F. A. Handler, and R. A. Matzner, *Scattering from black holes*. 1988.
- [111] N. Tsukamoto, “Deflection angle in the strong deflection limit in a general asymptotically flat, static, spherically symmetric spacetime,” *Physical Review D* **95** (2017), no. 6, 064035.